Engineering Structures 301 (2024) 117271

Contents lists available at ScienceDirect

Engineering Structures

journal homepage: www.elsevier.com/locate/engstruct

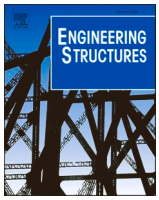

Seismic assessment and qualification of acceleration-sensitive nonstructural elements through shake table testing: Reliability of testing protocols and reliability-targeted safety factors

Danilo D'Angela [a,*], Gennaro Magliulo [a,b], Chiara Di Salvatore [a], Martino Zito [a]

[a] Department of Structures for Engineering and Architecture, University of Naples Federico II, Naples, Italy
[b] Construction Technologies Institute (ITC), National Research Council (CNR), Naples, Italy

ARTICLE INFO

Keywords:
Seismic assessment
Nonstructural elements
Shake table
Reliability
Safety factor

ABSTRACT

Shake table testing represents the best option for assessing and qualifying acceleration-sensitive nonstructural elements (NEs). Several testing protocols are defined in regulations and codes and implemented in the literature, but no commentaries or literature studies provide information regarding the expected reliability or recommend applicative safety factors. The study investigates the seismic reliability of shake table testing protocols for seismic assessment and qualification of acceleration-sensitive NEs. Numerical analyses are carried out considering an incremental procedure and modeling NEs as inelastic single degree of freedom (SDOF) systems, over a wide range of frequencies of interest and NE structural properties. Real floor motions recorded in instrumented reinforced concrete (RC) buildings are considered as a reference. The reliability is estimated considering several damage states and various floor motion sets. In particular, the seismic capacities associated with the real (shake table protocol) floor motions are considered as actual-demand (nominal-capacity) measures, and the demand to capacity margin is meant as the protocol overestimation of the NE capacity. In the light of the estimated protocol reliability, reliabiliy-targeted capacity safety factors are assessed, and applicative factor abaci and closed-form criteria are proposed.

1. Introduction

Nonstructural elements (NEs) are extremely vulnerable to seismic damage, as several post-survey studies demonstrated [1–5]. Moreover, the exposure associated with them is significant for ordinary buildings and might be extremely critical considering strategic and valuable facilities, which are required to be functioning in the aftermath of a seismic event or contain extremely valuable elements (e.g., [2,6–10]). Accordingly, seismic risk associated with NEs is likely to be high even in the case of low to moderate seismicity. Experimental tests represent the best option for estimating the seismic capacity and performance of NEs, and it is typically referred to for evaluation, qualification, and certification purposes (e.g., [11–15]). In particular, acceleration-sensitive NEs, i.e., elements that are sensitive to accelerations and inertial effects in terms of response and damage, are required to be assessed by means of dynamic tests, typically performed by means of shake table testing [9,11,16–21]. Codes and guidelines provide testing protocols for both seismic capacity estimation and qualification purposes. In particular, AC156 protocol [22] is referred to for seismic qualification purposes, whereas FEMA 461 [9] protocol has a broader scope and is also considered for fragility estimation; these protocols are intended to assess generic acceleration-sensitive elements, whereas other protocols are aimed at specific elements and equipment [23–26]. These protocols are widely used in the literature (e.g., [19,27–30]), but their reliability for seismic capacity and performance estimation is not known a priori, and it might be not satisfactory [31–33], especially for NEs that are not anchored (e.g., [34,35]). In many cases, the protocols do not provide background or technical information regarding the definition of the protocol target spectra (e.g., [31]). These concerns are stressed by the recent literature. For example, recent studies pointed out that the required response spectra (RRS) defined by AC156 protocol might be lower or significantly lower than the floor spectra associated with real buildings under earthquakes [27,36,37] and numerical analyses on buildings [32,38]. Furthermore, the compliance of an accelerogram

* Corresponding author.
E-mail address: danilo.dangela@unina.it (D. D'Angela).

https://doi.org/10.1016/j.engstruct.2023.117271
Received 28 June 2023; Received in revised form 10 November 2023; Accepted 29 November 2023

with target spectral response does not necessarily implies that the signal has an adequate severity, and enforcing spectrum-compatibility with relatively severe spectral responses might not be a sufficient condition for severity or representativeness of damage potential on NEs; this latter condition was investigated in [35] focusing on rocking-dominated elements. Finally, there is no information in the literature or within the relevant codes regarding the use of safety factors for the estimation of design measures of NE capacity from the direct experimental estimations.

The present study was developed in the framework of an extended seismic assessment campaign towards the enhancement of the current methods for a reliable estimation of the seismic demands on NEs and robust evaluation of their seismic capacity and performance [31,32,35,36,38,39]. The paper provides both methodology and results of an extensive reliability assessment of current shake table protocols for seismic assessment and qualification of (acceleration-sensitive) NEs. The methodologic framework defines the processes to evaluate (a) the reliability of engineering procedures as seismic capacity estimators and (b) reliability-targeted safety capacity factors associated with the implementation of the investigated seismic capacity estimators. The framework is applied considering (a) shake table testing as a seismic capacity estimator, with particular focus on testing protocols, and (b) a wide range of inelastic SDOF NEs as a case study. In particular, AC156 [17], FEMA 461 [9], and IEEE 693 [23] protocols are investigated, together with an enhanced version of AC156 and a protocol recently developed by Zito et al. [31]. The reliability indexes of the protocols are estimated by implementing incremental dynamic analyses of inelastic single degree of freedom (SDOF) systems, considering floor motions recorded in instrumented reinforced concrete (RC) buildings [40] as a reference. Five damage states (DSs) are considered for both damage assessment and reliability evaluation. The study finally provides reliability-targeted safety factors to be applied to the seismic capacities evaluated according to the investigated protocols by means of shake table testing, enforcing a given target reliability.

2. Methodology

2.1. Outline

The investigated engineering process is schematically depicted in Fig. 1a, and the methodology framework is depicted in Fig. 1b. The framework supplies (a) the reliability assessment of engineering procedures as seismic capacity estimators and (b) the reliability-targeted safety (capacity) factor estimation. Reference shake table protocols (STPs) were selected within current codes and relevant literature studies (Section 2.2); acceleration loading histories were defined considering both reference STPs (input generation and processing) and real records (input selection and processing) (Section 2.3). Case study NEs were identified favoring representativeness and generalizability (Section 2.4), and advanced numerical modeling was implemented, performing incremental dynamic analyses (IDAs, Section 2.5). Engineering demand parameter (EDP) and relevant DSs were defined (Section 2.6), and both damage (fragility) and reliability assessment were performed considering a newly defined perspective and according to literature methods (Section 2.7). In particular, the fragility assessment was functional to the reliability evaluation and is not discussed in this study since this falls beyond the scope. Finally, reliability-targeted safety factors were estimated according to a newly proposed method, favoring the applicative optimization (Section 2.8).

2.2. Reference shake table protocols

Shake table protocols (STPs) investigated in this study are AC156 [17], AC156w/o, FEMA 461 [9], IEEE 693 [23], Zito et al. [31], and 1 Hz-exception Zito et al. [31]; AC156w/o protocol is a modified (enhanced) version of AC156, whereas 1 Hz-exception Zito et al. protocol represents a peculiar application of Zito et al. [31], according to the exception criteria defined in the related study. AC156 protocol establishes the rules and criteria for seismic certification of NEs that have fundamental frequencies larger than 1.3 Hz. This protocol is considered

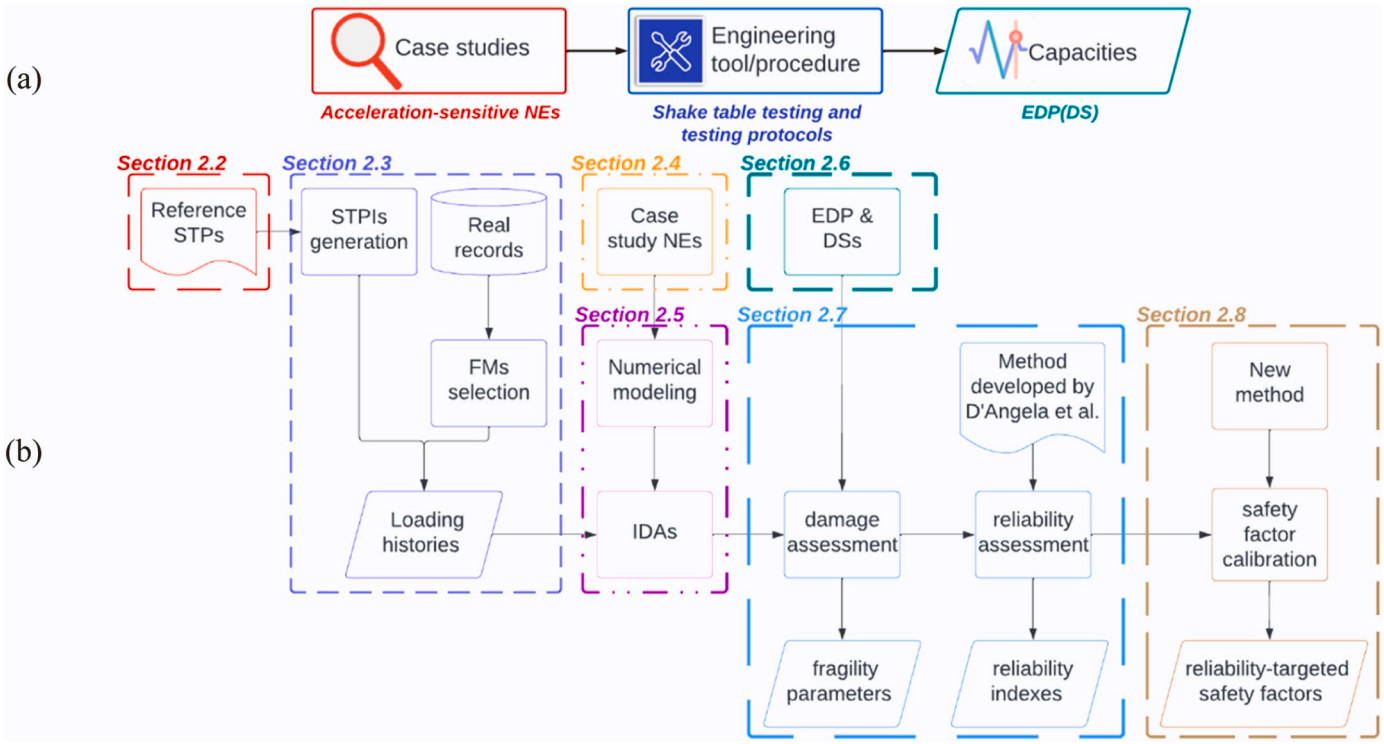

Fig. 1. (a) Investigated engineering process and (b) methodology framework. STP: shake table protocol; STPI: shake table protocol input; FM: floor motion; IDA: incremental dynamic analysis; NE: nonstructural element; EDP: engineering demand parameter; DS: damage state. D'Angela et al. [35].

as the international reference for seismic certification of NEs, in compliance with International Building Code [41] and ASCE 7 [11]. Two categories of tests are defined in the protocol, i.e., resonant frequency search and seismic simulation tests. The former tests are aimed at determining the resonant frequencies and damping of the test specimen, whereas the latter tests allow the assessment of the seismic capacity of the specimen, essential for the seismic certification. The input signal for the seismic simulation tests consists of nonstationary broadband random excitations having energy content ranging from 1.3 to 33.3 Hz and a bandwidth resolution equal to one-third for analog systems and one-sixth octave for digital ones. The input duration shall contain at least 20 s of strong motion. The input signal shall be compatible, in terms of test response spectrum (TRS), with RRS according to strict criteria. AC156 RRS is compliant with the design horizontal force provided by ASCE 7 [11], and this is defined by two acceleration thresholds: A_{FLX}, i.e., plateau spectral ordinate over 1.3–8.3 Hz, and (b) A_{RIG}, i.e., spectral ordinate at 33.3 Hz; RRS is log-linear between 8.3 and 33.3 Hz. RRS is also defined for frequencies lower than 1.3 Hz, but this is not to be considered for spectral compatibility analysis. RRS is defined for horizontal and vertical directions according to the formulations provided for $\{A_{FLX\text{-}H}, A_{RIG\text{-}H}\}$ and $\{A_{FLX\text{-}V}, A_{RIG\text{-}V}\}$, respectively. The key parameters for determining RRS are S_{DS}, i.e., design spectral response acceleration parameter at short periods, and z/H, i.e., ratio between the height location of NE (z) and the building height (h).

AC156 protocol assumes an upper bound limit for $A_{FLX\text{-}H}$, equal to 1.6 S_{DS}. This limitation was derived from the provisions for the evaluation of the seismic demand force on NEs (ASCE 7). $A_{FLX\text{-}H}$ reduction associated with this limitation increases linearly from z/H equal to 0.3 (null reduction) to z/H equal to one (47% reduction). This limitation might significantly affect the severity of the compliant seismic input and might even result in unsafe capacity estimations, as recent studies pointed out [27,35,38,39], e.g., Petrone et al. [38] proved that such a limitation generates RRS that might underestimate the floor response spectra related to a representative set of generic frame structures. Accordingly, a modified version of AC156 protocol, namely AC156w/o, was considered in this study. In particular, AC156w/o RRS coincides with AC156 RRS without applying the abovementioned limitation to $A_{FLX\text{-}H}$, and AC156w/o signal generation procedure is the same implemented for AC156.

FEMA 461 protocol provides methods for seismic evaluation of structural and NEs, identifying shake table testing as the most preferred method for assessment of acceleration-sensitive NEs. The shake table testing protocol is designed for testing elements that are sensitive to the velocity and dynamic effect of motion imparted at a single point of attachment. The seismic performance of the test specimen is evaluated under input motions of increasing intensities representative of the motion at the single level of a building structure on which the test specimen is located. Seismic inputs used to assess the capacity of NEs were developed by Wilcosky et al. [42]: the test input consists of a 60-s narrowband random sweep excitation signal, with a center frequency of the sweeps ranging from 32 Hz to 0.5 Hz, at a rate of six octaves per minute, having a bandwidth resolution equal to one-third octave. FEMA 461 does not provide the RRS, but only some representative cases, and generic spectral indications: TRS should be relatively smooth with the acceleration response spectra amplitude equal to 1 g within 2 and 32 Hz and with a uniform displacement response spectrum below 2 Hz. The spectral ordinate of the TRS at the resonant frequency of the NE (i.e., $S(T_a)$) is considered as an intensity parameter. The protocol also defines a procedure for the generation and the filtering of the shake table input; however, the use of the provided signals is implicitly suggested.

IEEE 693 protocol establishes criteria for seismic design and qualification of electrical substation equipment, according to three seismic qualification levels (low, moderate, and high). Qualification levels are defined according to zero period acceleration (ZPA) of RRS, i.e., high and moderate levels are associated with horizontal ZPA equal to 1.0 and 0.5 g, respectively, whereas no specific ZPA value is associated with low level. IEEE 693 RRS does not account for the influence of the of hosting building, which can be considered by amplifying RRS by 2.5. The input signal of the seismic simulation tests shall have a duration of at least 20 s of strong motion. Theoretical TRS (i.e., related to assigned signal) shall be computed at 5% damping and shall meet RRS from the lower corner point frequency of the target response spectra (1.1 Hz). Unlike other protocols, IEEE 693 supplies different spectrum-compatibility rules for theoretical and recorded inputs. The protocol provides several spectrum-compatible seismic inputs, in particular, Takhirov et al. [43] developed several time histories according to IEEE 693 protocol: they were generated considering different earthquake types, i.e., crustal, subduction, and artificial ones.

The protocol defined by Zito et al. [31] provides criteria for seismic qualification and certification of (acceleration-sensitive) NEs that have fundamental frequencies greater than 1.0 Hz. The loading program consists of a series of dynamic tests, including both dynamic identification tests and seismic performance evaluation tests. This protocol considers two approaches: specific performance level qualification and extensive qualification. The former is intended to verify whether the component fulfills a specific performance level, associated with a target level of a relevant (seismic) intensity parameter defined by regulations or codes. The latter qualification consists in an incremental testing procedure encompassing low to high seismic intensities and minor to major damage states. Zito et al. RRS was derived from the formulation provided by the Italian building code [44,45], which was developed in [32] and assessed in several studies (e.g., [46,47]); in particular, RRS was defined by implementing a general and site-building independent approach. The use of Zito et al. protocol favors (a) generalizable, (b) representative, and (c) consistent assessment and qualification procedures. In particular, (a) the generalizability is associated with the possibility to (i) consider a wide range of buildings and (ii) implement the protocol definition procedure considering different RRS formulations (e.g., specific site and building conditions), (b) the representativeness is related to the characteristic and exemplifying nature of both protocol and signal development procedure, and (c) the consistency is meant as the compliance with consolidated procedures and formulations and with the scientific background. Zito et al. [31] also provides exception criteria to be applied when the signal cannot be adequately reproduced by the shake table due to instrumental issues, e.g., exceeded peak displacement capacities or instrumental dynamic resonance issues, despite consolidated filtering procedures have been implemented. In this study, it is hypothesized that frequencies in the vicinity of 1.0 Hz are critical for the testing facility, and Zito et al. exceptions are applied accordingly, defining 1 Hz-exception Zito et al. protocol. It should be mentioned that the investigated exception might be consistent with several testing facilities since low frequencies are often critical in terms of spectrum-compatibility and signal reproduction by shake tables [43,48]. Further details regarding the definition of the exception signals are omitted for the sake of brevity, and the reader is referred to [31].

2.3. Loading histories

Two types of acceleration records were selected for the numerical analyses: floor motions (FMs) and shake table protocol inputs (STPIs). FMs were provided by Center for Engineering Strong Motion Data (CESMD) database [40] and consist in real accelerograms recorded in US instrumented buildings. FMs are related to ground motions having peak ground acceleration (PGA) not smaller than 0.05 g, and they are always associated with higher intensity response over the building floors (mostly recorded at the roof level). The case study buildings consist in RC buildings designed within 1923 – 1975. In particular, 18 FMs were considered in this study, deriving them from the 24 FMs selected by D'Angela et al. [39]. In particular, FMs #4, #8, #11, #16, #20, and #24 considered in this latter study were not included in the present study since a pilot study (carried out by the authors) showed that these records

were extremely mild for the case study NE models. The considered FM set (FM#1 to FM#18) is widely representative in terms of (a) recorded PGA and peak floor acceleration (PFA) distribution, (b) near and far field records, and (c) low-, medium-, and high-rise buildings. The FM subsets considered in the study are identified as NFFM (near field floor motion), FFFM (far field floor motion), and SFM (strong floor motion) sets; SFM set includes inputs associated with PGA larger than or equal to 0.20 g. For the sake of brevity, further FM details are not reported in this paper since they are provided in the abovementioned study.

STPIs are artificial inputs derived compliant with the most authoritative STPs for seismic evaluation, qualification, and certification of acceleration-sensitive elements. STPIs were generated or derived according to STPs described in Section 2.2. Seven acceleration time histories were generated according to AC156 (AC set: AC#1 to AC#7), according to [16,48]; z/H was set equal to one to consider the most severe NE location condition as well as to consider the highest upper cut spectral limitation [27,35]. Seven inputs were generated according to AC156w/o (ACmod set: ACmod#1 to ACmod#7), i.e., considering the procedure related to AC156 without applying the $A_{FLX\text{-}H}$ upper bound limit. Three inputs developed according to FEMA 461 were considered (FEMA set: FEMA#1 to FEMA#3): FEMA#1 and FEMA#2 were provided by FEMA 461 (i.e., recommended longitudinal and transversal records) and FEMA#3 was generated in D'Angela et al. [35], according to the commentary of FEMA 461 and the procedure developed by Wilcoski et al. [42]. It was verified that AC, ACmod, and FEMA set signals were compatible with representative shake table testing facilities, considering a spectral acceleration response at rigid periods equal to 1.0 g as a reference. In particular, the signals met the capacity limits of the shake tables of the University of Naples (e.g., [20]), and the most severe limitations were associate with peak displacement and upper frequency limit (capacity thresholds equal to 250 mm and 50 Hz, respectively).

Ten acceleration time histories were selected according to IEEE 693 (IEEE#1 to IEEE#10 corresponding to TestQke4IEEE5–1X, TestQke4IEEE5–2X, TestQke4IEEE5–2Y, TestQke4IEEE5–4X, TestQke4IEEE5–4Y, TestQke4IEEE5–6X, TestQke4IEEE5–6Y, TestQke4IEEE5–7Y, TestQke4IEEE5–8X, and TestQke4IEEE5–8Y, respectively), also considering the study by Takhirov et al. [43]. IEEE#1 to IEEE#5 inputs were obtained by considering empirical time histories as a baseline (i.e., El-Centro, CA (1940), Landers, CA (1992), and El Mayor-Cucapah, Mexico (2010)), whereas the others were artificially generated. Seven IEEE 693 set inputs (IEEE#4 to IEEE#10) were selected among the filtered versions of IEEE-spectrum compatible time histories and with peak displacements limitations of 200 mm, developed by Takhirov et al. [43]. This limit was considered to be compliant with the abovementioned shake table limitations. IEEE#1 to IEEE#3 were derived by IEEE 693-compliant signals but were filtered in this study considering a band-pass Butterworth filter over the range of frequency 0.5 ÷ 35 Hz to meet the same displacement limit [49]. Seven inputs were developed according to Zito et al. protocol, according to the procedure defined in [31], not reported here for the sake of brevity. In particular, the signals were artificially generated as nonstationary random signals with an energy content ranging from 1.0 to 32.0 Hz and a duration of 30 s. The theoretical spectra of the signal inputs were matched to the RRS defined with PGA equal to 0.4 g and the height ratio z/H equal to one. RRS was developed by generalizing and extending the formulation of the seismic demands on NEs provided by Italian building code [32,44,45]. The acceleration time histories were filtered with a band-pass filter to be compatible with the facilities limits previously described [49].

Fig. 2 shows the spectral acceleration response (Sa) as a function of frequency (f_a) associated with FM and STPI sets, assuming PFA equal to 1.0 g. Both (a) median and (b) 84th percentile spectra are depicted. It should be specified that comparing the input set spectral responses considering a fixed value of PFA (e.g., 1.0 g) highlights the spectral amplification due to the different protocols for a given level of seismicity and NE location. As a matter of fact, PFA can be meant as the combination of a seismicity measure (PGA) and of a building amplification measure (PFA/PGA) (e.g., [39]). Furthermore, PFA was also considered as an intensity measure (IM) for the IDA procedure.

For a more technical assessment, a comparison among RRS associated with international protocols is depicted in Fig. 3 [31], considering two comparison criteria: (a) PGA equal to 0.50 g and (b) spectral ordinate at 32 Hz equal to 1.0 g. In addition to the protocols investigated in this study, ISO 13033 [50], GR-63 [25], RG-1.60 [51], and IEC 60068 [52] protocols are considered [12]. When applicable, both z/H equal to

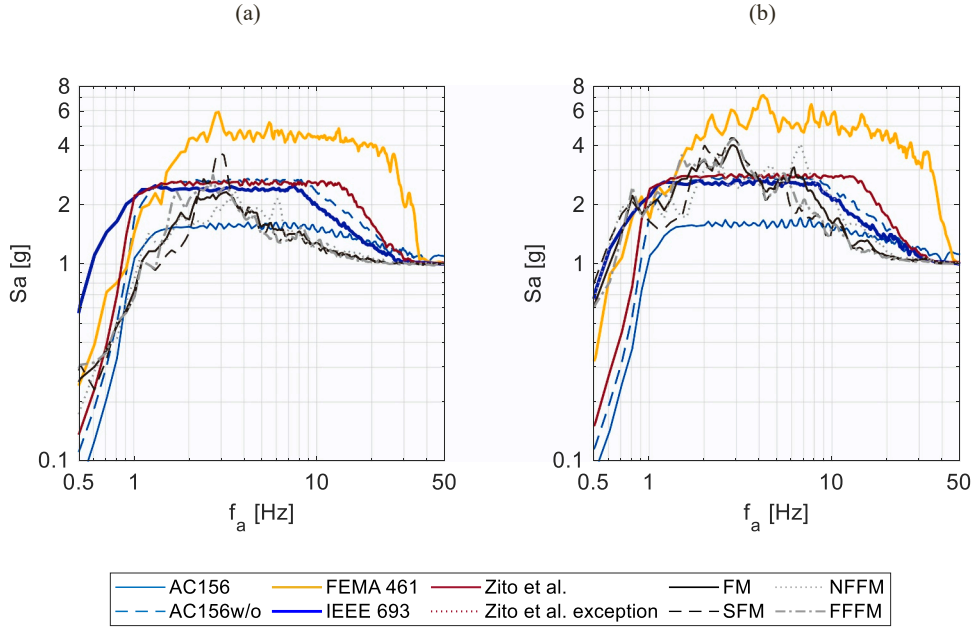

Fig. 2. Spectral acceleration response (Sa) over frequency (f_a) associated with floor motion (FM) and shake table protocol input (STPI) sets: (a) median curves and (b) 84th percentile curves. The spectra were computed considering peak floor acceleration (PFA) equal to 1.0 g.

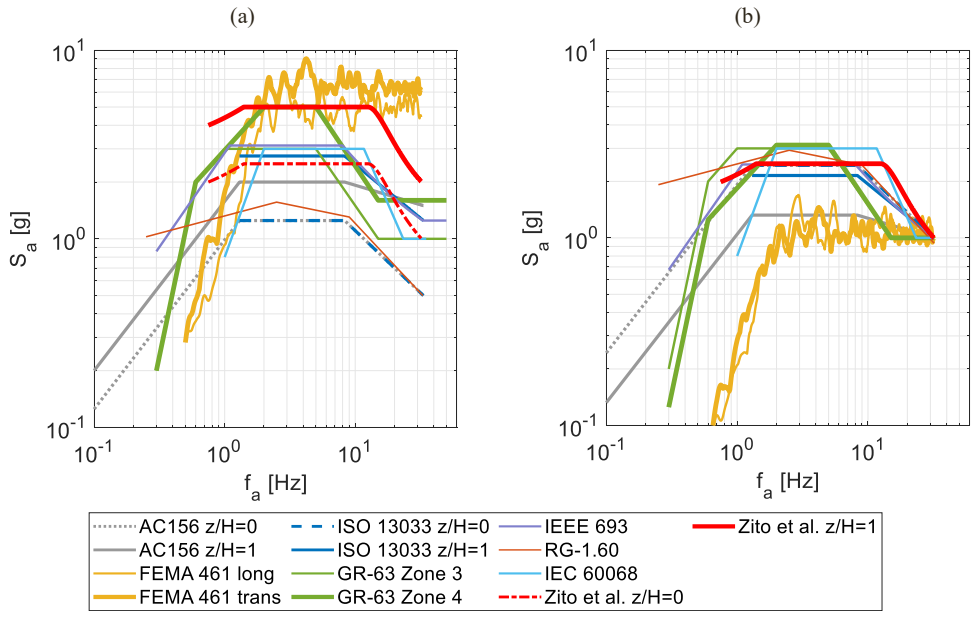

Fig. 3. Spectral acceleration response (Sa) over frequency f_a associated with required response spectra (RRS) of shake table protocols (STPs), compared considering (a) peak ground acceleration (PGA) equal to 0.50 g and (b) spectral ordinate corresponding to 32 Hz equal to 1.0 g [31].

zero and one conditions are plotted, and for GR-63 protocol, both Zone 3 and Zone 4 spectra are shown since they are both compatible with the considered intensity level.

2.4. Case study models

NEs of interest are acceleration-sensitive elements that can be modeled by SDOF systems. In particular, case studies consist in cantilever elements with lumped mass at the free end. This model was chosen since it is representative of the dynamic behavior of wide range of acceleration-sensitive NEs, such as operating lights, projectors, antennas, base-anchored cabinets, and museum artifacts. Fig. 4 depicts representative examples of critical NEs that can be modeled by SDOF systems, parts of historical structures and related supports exposed at the National Archeological Museum of Naples (MANN), Italy. Indeed, acceleration-sensitive NEs are generally meant to be SDOF systems in the literature (e.g., [32,53,54]), and the assessment methodology, including seismic demand estimation, is based on SDOF hypotheses and spectral responses [11,45,55].

A set of 12 models was considered to account for various NEs over a wide range of elastic frequencies and structural properties. All models were made of steel S275 square hollow sections (SHS). In fact, acceleration-sensitive NEs are often made by a resisting system (structure) composed by steel elements, often tubular sections or profiles. Table 1 reports the structural details of the case study models, including the elastic frequency (f_a); f_a was computed considering the theoretical estimation of a SDOF system frequency, considering the lateral stiffness and the applied mass. The models were defined by varying cross-section dimensions (i.e., size b and thickness t), mass m, and elevation height h. In particular, the models cover a wide range of elastic frequencies (approximately from 1 to 9 Hz) that is representative of most NEs (e.g., [11,56]). In particular, four ranges of elastic frequency were defined, i.e., (range I) ~1.0 Hz, (range II) ~1.5 Hz, (range III) ~3.0 Hz, and (range IV) > ~3.0 Hz; three models were defined for each range, i.e., {M1a,M1b,M1c}, {M2a,M2b,M2c}, {M3a,M3b,M3c}, and {M4a,M4b,M4c}, corresponding to ranges I, II, III, and IV, respectively. The investigated elements were assessed with regard to the global instability conditions, and the demand to capacity ratios were significantly lower than the unity, considering the applied mass as a reference. Even though elements with relatively high fundamental frequencies are investigated in the study, it should be specified that the investigated models are not meant to be representative of relatively rigid NEs such as systems that are governed by sliding and rocking response. For the abovementioned elements, specific models should be referred to (e.g., [39,57,58]).

Table 1
Structural details of the investigated models.

Model ID	range [-]	f_a [Hz]	f_a [Hz]	b [mm]	t [mm]	h [m]	m [t]
M1a	I	~1.0	1.02	70	3.0	4.50	0.10
M1b			1.03	60	3.0	2.50	0.35
M1c			1.13	50	2.5	3.00	0.08
M2a	II	~1.5	1.48	70	3.0	3.50	0.10
M2b			1.52	60	3.0	2.50	0.16
M2c			1.52	60	2.5	3.00	0.08
M3a	III	~3.0	2.97	70	3.0	2.20	0.10
M3b			3.04	60	3.0	2.50	0.04
M3c			3.06	90	3.0	3.00	0.08
M4a	IV	> ~3.0	5.86	70	3.0	1.40	0.10
M4b			7.34	80	4.0	1.50	0.10
M4c			9.02	70	3.0	1.05	0.10

Fig. 4. Parts of historical structures and related supports exposed at the National Archeological Museum of Naples (MANN), Italy, which can be reasonably modeled by single-degree-of-freedom (SDOF) systems.

2.5. Numerical modeling and analysis

The case study models were implemented in OpenSees [59] considering a lumped plasticity approach. In particular, each model consists in a series of an elastic vertical cantilever element and an inelastic moment-rotation spring, defined over three nodes (Fig. 5a). In particular, (a) the spring was defined between a fixed node (node 1) and a (free) node (node 100) having the same coordinates of node 1 and (b) the vertical element was assigned between node 100 and a (free) node (node 2) having elevation coordinate equal to h and other coordinates equal to the ones of nodes 1 and 100.

The elastic and spring elements were modeled by an elasticBeamColumn element and a zerolength element, respectively. The moment-rotation backbone and deterioration parameters of the spring element were determined according to Lignos and Krawinkler [60], who calibrated the Ibarra-Medina-Krawinkler (IMK) model [61,62] for steel SHS columns, considering more than 120 literature tests on columns (including both cantilever columns and columns fixed at both ends). In particular, uniaxialMaterial ModIMKPeakOriented response was assigned to the zerolength element. The backbone is defined by yielding, capping and ultimate moment-rotation conditions, whereas cyclic deterioration is modeled according to an energy dissipation criterion, through the cumulative rotation capacity (Λ). Four deterioration modes can be implemented: strength, stiffness, post-capping stiffness, and reloading stiffness. Empirical formulations are provided by Lignos and Krawinkler [60] for the estimation of pre-capping rotation (θ_p), i.e., the difference between the capping and the yielding rotation (Eq. (1)), post-capping rotation (θ_{pc}), i.e., the difference between the ultimate rotation and the capping one (Eq. (2)), and cumulative rotation capacity (Λ), i.e., the ratio between the reference hysteretic energy dissipation capacity (typical of the system) and the pre-capping rotation (Eq. (3)). In particular, N is the applied axial load, N_y is the yield axial load, F_y is the expected yield strength (in MPa), and c is a factor for unit conversion, which is equal to one if F_y is expressed in MPa. In this context, N was assumed to be equal to the mass applied on the top of the NE model. The denominator of the fourth factor, i.e., 380, aims at normalizing the factor since it represents the nominal yield strength of steel typically used for tubular columns in Japan.

$$\theta_p = 0.614\left(\frac{b}{t}\right)^{-1.05}\left(1-\frac{N}{N_y}\right)^{1.18}\left(\frac{c\cdot F_y}{380}\right)^{-0.11} \quad (1)$$

$$\theta_{pc} = 13.82\left(\frac{b}{t}\right)^{-1.22}\left(1-\frac{N}{N_y}\right)^{3.04}\left(\frac{c\cdot F_y}{380}\right)^{-0.15} \quad (2)$$

$$\Lambda = 3012\left(\frac{b}{t}\right)^{-2.49}\left(1-\frac{N}{N_y}\right)^{3.51}\left(\frac{c\cdot F_y}{380}\right)^{-0.20} \quad (3)$$

The provided equations are applicable within parameter ranges provided in Equations (4); the case study models are compatible with the abovementioned applicability conditions.

$$20 \le \frac{b}{t} \le 60 \quad (4.1)$$

$$0 \le \frac{N}{N_y} \le 0.5 \quad (4.2)$$

$$276\ \text{MPa} \le F_y \le 500\ \text{MPa} \quad (4.3)$$

Yielding moment (M_y) and yielding rotation (θ_y) were evaluated considering the elastic properties of the cross-sections, according to available handbooks. A strength reduction stabilization was taken into account by assuming a residual strength threshold (M_r), as a fraction of M_y, i.e., $M_r = k\ M_y$, with $k = 0.25$ (experimentally calibrated [60,63]). The global backbone curves (in-series members) related to the investigated models are depicted in Fig. 4b considering moment-rotation response. Only the positive branch is illustrated in Fig. 4b (the response is symmetric). It is worth noticing that backbone curves related to M1b, M2b, and M3b are overlapped since the models only differ in terms of mass (and other mechanical parameters are the same).

The member backbone response is associated with the in-series response of the elastic and spring elements (Fig. 5c). In order to avoid convergence issues, the spring was modeled as elastic-plastic instead of a perfectly plastic spring, according to [64–66], as it is described in the following. The elastic element and spring elastic stiffness were set by enforcing the following conditions: (a) spring stiffness equal to n times the elastic element one and (b) in-series member stiffness corresponding to the backbone derived from the abovementioned formulation; n was assumed to be equal to ten according to the relevant literature [64,66,67]. Fig. 5c depicts an example of backbone curves, expressed as moment-rotation response, associated with single series elements (elastic cantilever and elastic-plastic spring) and in-series member.

Second order geometric nonlinearities, namely P-Δ effects, were implemented in the analyses. Rayleigh damping was assumed in the

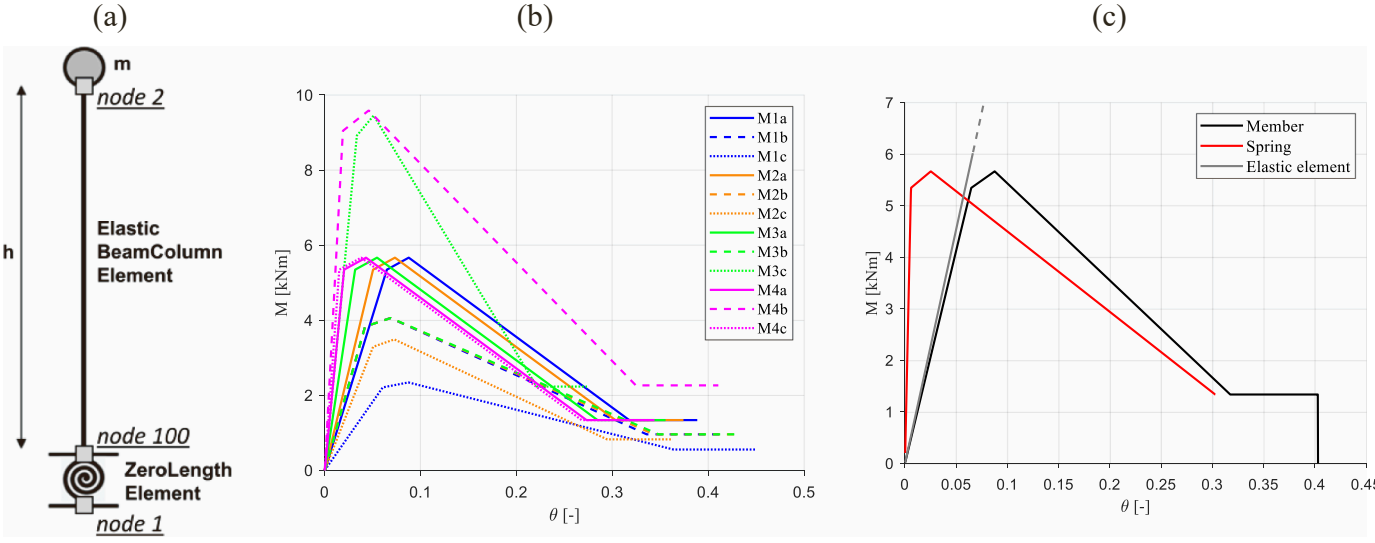

Fig. 5. Depiction of the numerical models: (a) schematic of the implemented in-series system, (b) moment-rotation (M-θ) backbone curves related to the investigated models, and (c) example of M-θ response of elastic/spring elements and in-series member.

model (mass and initial tangent stiffness-proportional), considering a damping ratio equal to 5% [64]. The damping was only assigned to the elastic element in order to ease the analysis convergence (see [68]). IDAs [69] were carried out by scaling PFA from 0.05 g to component failure, through increments of 0.05 g. Structural resurrection [69] was not accounted for. The numerical results and IDA curves are not reported and discussed in this paper since this is beyond the scope of the study.

2.6. Engineering demand parameter and damage states

The damage of the systems was assessed considering the horizontal displacement of the concentrated mass Δ as an EDP. Five DSs were defined according to Fig. 6, i.e., DS1, DS2, DS3, DS4, and DS5 achieved when Δ exceeds or equals the related displacement capacity thresholds Δ_{DS1}, Δ_{DS2}, Δ_{DS3}, Δ_{DS4}, and Δ_{DS5}. In particular, Δ_{DS1} is halved yielding displacement, Δ_{DS2} is yielding displacement, Δ_{DS3} is capping displacement, Δ_{DS4} is displacement associated with strength drop of 20% from the capping condition, and Δ_{DS5} is the smallest displacement associated with residual strength (or onset of perfectly-plastic response). Table 2 reports the displacement capacities associated with the investigated models, considering the global member response estimated through nonlinear static analyses (pushover curves) including P-Δ effects. Considering the response of the spring instead of the global member for the damage assessment would not correctly account for the elastic contribution to the deformations, since the spring is provided with a conventional aliquot of the global elastic stiffness.

Considering the modeled NEs (and not the hypothetical hosting facility), DS1 is representative of full functioning, DS2 is associated with damage limitation, DS3 is correlated with life safety, and DS4 is related to a relatively early failure condition, and DS5 is representative of a complete failure. Obviously, the performance levels to be guaranteed, the relevant limit states, and the associated seismic demand depend on the reference regulation and case study facility, and it is worth specifying that the present study aims at performing damage assessment rather than safety assessment.

2.7. Damage and reliability assessment

2.7.1. Fragility analysis

Damage assessment was carried out through estimation of fragility curves, associated with the response of the investigated models (Section 2.4) subjected to the analysis loading history sets (Sections 2.2 and 2.3)

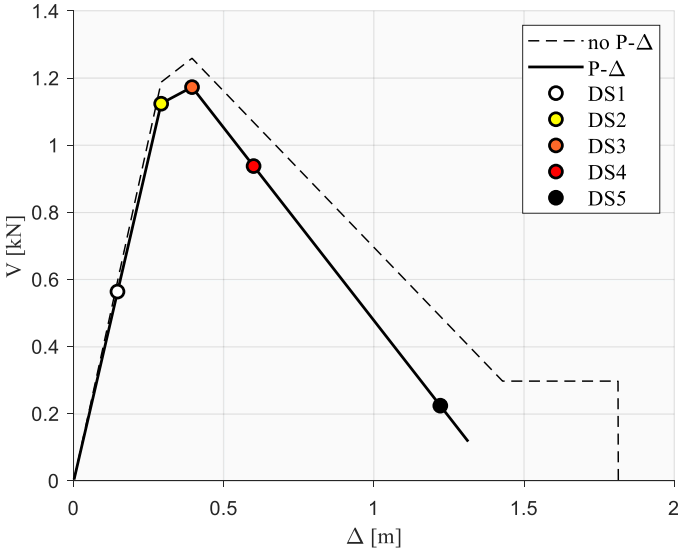

Fig. 6. Schematic definition of damage states (DSs) considering the P-Δ effects on the pushover curve (V vs. Δ).

Table 2
Displacement capacities associated with investigated damage states (DSs), considering the global member response and including P-Δ effects.

Model ID	Δ_{DS1} [m]	Δ_{DS2} [m]	Δ_{DS3} [m]	Δ_{DS4} [m]	Δ_{DS5} [m]
M1a	0.146	0.291	0.394	0.599	1.221
M1b	0.052	0.105	0.171	0.257	0.515
M1c	0.091	0.181	0.262	0.407	0.847
M2a	0.088	0.176	0.256	0.427	0.945
M2b	0.052	0.105	0.172	0.297	0.674
M2c	0.076	0.151	0.218	0.357	0.778
M3a	0.035	0.070	0.120	0.237	0.591
M3b	0.052	0.105	0.172	0.338	0.841
M3c	0.050	0.100	0.153	0.278	0.659
M4a	0.014	0.028	0.060	0.138	0.376
M4b	0.014	0.028	0.069	0.172	0.486
M4c	0.008	0.016	0.040	0.100	0.281

in the framework of the performed analyses (Section 2.5). In particular the fragility is estimated assuming an IM-based lognormal model (Porter method A) [70]; PFA was considered as an IM, and Δ was used as an EDP (Section 2.6). The fragility was computed considering DS1 to DS5 (Section 2.6). The only record-to-record uncertainty was considered in this study. The fragility median value and logarithmic standard deviation are defined x_m and σ, respectively. The estimated fragility curves are not reported and discussed in this paper since these were processed to evaluate the reliability of the investigated protocols (Section 2.7.2); moreover, the fragility assessment falls beyond the scope of this paper.

2.7.2. Reliability evaluation

The reliability of the investigated protocols was assessed by implementing the methodology developed in [35]. In particular, the reliability index β was computed according to second-level first-order reliability method (FORM) [71]. In particular, capacity (R) and demand (S) measures corresponded to capacities associated with FM (actual capacities) and protocol (nominal capacities), respectively, and demand to capacity margin (Z) corresponded to protocol overestimation of the capacity in relation to FM capacity (or equivalently, nominal overcapacity in relation to actual capacity). Accordingly, β accounts for the reliability of the protocol, considering FM capacities as a reference. P_f is defined by Φ(-β), where Φ is the cumulative standard normal distribution and represents the failure probability associated with the protocol, i.e., the probability that the capacity assessed considering the protocol exceeds the capacity associated with FM, or equivalently the probability that the margin between the protocol and FM capacity estimation is positive. R and S were assumed to be uncorrelated, and the probabilistic distributions of R and S were assessed considering the estimated fragility functions. In particular, β was computed by means of Eq. (5) [35,71].

$$\beta = \frac{\ln\left(\frac{x_{m,R}}{x_{m,S}}\right)}{\left(\sigma_S^2 + \sigma_R^2\right)^{0.5}} \quad (5)$$

2.8. Estimation of reliability-targeted safety factors

In earthquake engineering, the concept of risk- and reliability-targeted design and assessment was widely applied to structures and infrastructures in the last few decades. However, no studies or applications, to the authors' knowledge, extended these approaches to NEs, even though these latter elements are often associated with critical seismic risk. A major step towards a reliability-targeted design and assessment of NEs was carried out in this study. Safety factors were developed for performing safety assessment of NEs according to first-level reliability methods (semi-probabilistic approach). This allows the implementation of more reliable assessment procedures among practitioners and professionals. In particular, the study develops safety factors

(k) to be applied to the capacities estimated according to the protocols, explicitly calibrated to achieve given levels of reliability associated with the implementation of the investigated protocols. Even though these factors are to be applied to capacities, they also account for the uncertainty associated with seismic demand, as it will be cleared in the following.

Eq. (6) was used to estimate k as a function of a given target reliability index (failure probability), defined $\overline{\beta}$ ($\overline{P_f}$), and fragilities associated with FM and protocol capacities, corresponding to R and S measures, respectively.

$$k = \exp\left(\overline{\beta} \quad \left(\sigma_S{}^2 + \sigma_R{}^2\right)^{0.5}\right) \left(\frac{x_{m,S}}{x_{m,R}}\right) \tag{6}$$

Eq. (6) was derived by explicitly giving k from Eq. (7), which corresponds to the reliability index associated with a set of protocol capacities having median and logarithmic standard deviation equal to $\overline{x_{m,S}}$ and $\overline{\sigma_S}$, respectively, where $\overline{x_{m,S}}$ is equal to $x_{m,S}/k$ and $\overline{\sigma_S}$ is equal to σ_S.

$$\overline{\beta} = \frac{\ln\left(\frac{x_{m,R}}{\overline{x_{m,S}}}\right)}{\left(\overline{\sigma_S}^2 + \sigma_R{}^2\right)^{0.5}} \tag{7}$$

As a matter of fact, if all members of protocol capacity set (S) are divided by k (i.e., to apply the safety factor to the capacity measures), the median of the lognormal distribution related to the resulting capacity set ($\overline{S}$) is equal to the median value of S set divided by k ($\overline{x_{m,S}} = x_{m,S}/k$), whereas the logarithmic standard deviation of $\overline{S}$ set is equal to the logarithmic standard deviation of the unmodified protocol capacity set ($\overline{\sigma_S} = \sigma_S$). Accordingly, Eq. (6) allows identifying the value of k that determines the achievement of a target value of β (i.e., $\overline{\beta}$) for the related case study application (DS, model properties, and protocol). Therefore, k represents the reliability-targeted safety factors to be applied to capacity estimations related to the investigated protocols (S) to estimate the reliability-targeted protocol capacities ($\overline{S}$).

Fig. 7 depicts k as a function of $x_{m,S}/x_{m,R}$ and $\sigma_S{}^2 + \sigma_R{}^2$ or σ_S (for multiple values of σ_R), assuming $\overline{\beta}$ equal to 0.5, 1.0, and 2, which correspond to $\overline{P_f}$ approximately equal to 31%, 16%, and 7%, respectively. As it can be easily observed in Fig. 7, an increase in σ_S (or σ_R) or in $\left(\sigma_S{}^2 + \sigma_R{}^2\right)^{0.5}$ is associated with an increase in terms of k corresponding for given $x_{m,S}/x_{m,R}$, and the higher the target $\overline{\beta}$ is, the larger is the magnitude of the k growth; or equivalently, an increase in σ_S (or σ_R) or in $\left(\sigma_S{}^2 + \sigma_R{}^2\right)^{0.5}$ corresponds in a decrease of the requested $x_{m,S}/x_{m,R}$

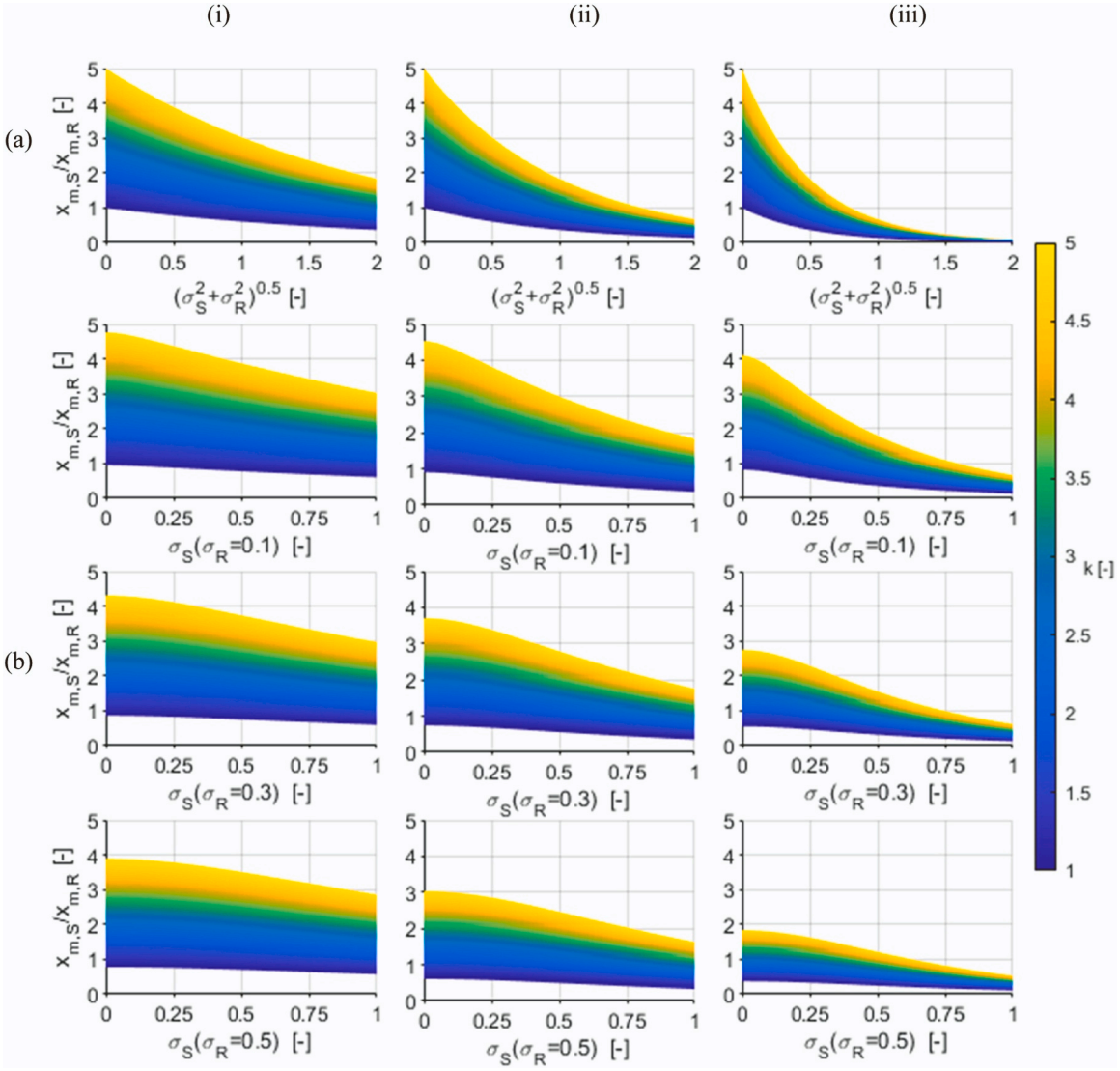

Fig. 7. Safety factor (k) expressed as a function of $x_{m,S}/x_{m,R}$ and (a) $\sigma_S{}^2 + \sigma_R{}^2$ and (b) σ_S (considering σ_R equal to 0.1, 0.3, and 0.5), assuming $\overline{\beta}$ equal to (i) 0.5, (ii) 1.0, and (iii) 2, corresponding to $\overline{P_f}$ approximately equal to 31%, 16%, and 7% (Eq. (6)).

ratio associated with a given target k, which is growing in magnitude as $\overline{\beta}$ increases.

Since k values were calibrated considering uncertainty associated with both capacity and demand measures, the reduction of the nominal capacity due to the application of the estimated safety factor also accounts for the increase of the seismic demand associated with a reasonable uncertainty assessment. In other words, the uncertainty associated with the seismic demand is included within the safety factor to be applied to the capacity. Analogously, it could be reasonably assumed that an aliquot of the safety factor is associated with the contribution of the demand uncertainty. Obviously, the estimated k values are associated with the sources of uncertainties accounted for in the paper (i.e., record-to-record).

It can be easily found that Eq. (7) can be expressed as a function of $\overline{\beta}$, β, and $\sqrt{\sigma_S^2+\sigma_R^2}$ as it is reported in Eq. (8) and depicted in Fig. 8.

$$k = \exp\left[(\overline{\beta}-\beta)\left(\sigma_S^2+\sigma_R^2\right)^{0.5}\right] \quad (8)$$

The factor $(\overline{\beta}-\beta)$ represents the reliability increment needed to reach the target reliability starting from the estimated reliability index, and this has a primary role on the determination of k; the influence of the factor $\left(\sigma_S^2+\sigma_R^2\right)^{0.5}$ was already discussed regarding Fig. 7. Three representative cases can be evidenced:

- a significantly unreliable protocol (e.g., $(\overline{\beta}-\beta)$ equal to 3) is associated with relatively small k values (e.g., equal to 1.8), if the dispersion of the protocol is relatively reduced (e.g., $\left(\sigma_S^2+\sigma_R^2\right)^{0.5}$ equal to 0.20)) (e.g., point A in Fig. 8);
- a protocol with the same reliability of the abovementioned one is associated with significantly larger k values (e.g., equal to 3.3) if $\left(\sigma_S^2+\sigma_R^2\right)^{0.5}$ increases (e.g., doubles) (e.g., point B in Fig. 8);
- a protocol significantly more reliable that the abovementioned ones (e.g., $(\overline{\beta}-\beta)$ equal to 1.5) is associated with significantly larger k values (e.g., equal to 4.5) if the dispersion is relatively large (e.g., $\left(\sigma_S^2+\sigma_R^2\right)^{0.5}$ equal to 1) (e.g., point C in Fig. 8).

$\overline{\beta}$ equal to one might represent a first tentative threshold for defining a relatively safe and not critically conservative target threshold [35]. It is worth specifying that the defined methodology is generally applicable, and different $\overline{\beta}$ ($\overline{P_f}$) can be selected according to the desired level of safety and significance of element and facility. For each protocol, k values were assessed as a function of DSs and models. Finally, fitting curves were provided to estimate k as a function of the elastic frequency of NEs.

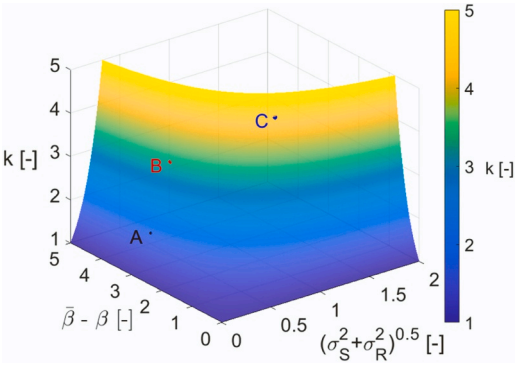

Fig. 8. Safety factor (k) expressed as a function of $(\overline{\beta}-\beta)$ and $\left(\sigma_S^2+\sigma_R^2\right)^{0.5}$ (Eq. (8)). Points A, B, and C have $[\left(\sigma_S^2+\sigma_R^2\right)^{0.5}, (\overline{\beta}-\beta), k]$ coordinates equal to (0.2,3,1.8), (0.4,3,3.3), and (1,1.5,4.5).

3. Reliability index and failure probability

Fig. 9 shows the reliability index β related to the investigated protocols considering FM set as a reference, estimated for all investigated models and DSs. The failure probability (P_f) associated with estimated β is also depicted (Fig. 10) for the sake of completeness. The results related to other FM sets are reported in the Appendix, but they are also discussed in this section.

β (P_f) depends on FM set (FM, STF, NFFM, and FFFM), DS (DS1 to DS5), model frequency ranges (I ($f_a = 1.0$ Hz), II ($f_a = 1.5$ Hz), III ($f_a = 3.0$ Hz), and IV ($f_a > 3$ Hz, i.e., $f_a = 5.9, 7.3, 9$ Hz)), models within model frequency range and protocol. The key results regarding the abovementioned features are discussed with regard to β (Fig. 9) considering the FM sets (Section 3.1), the models (Sections 3.2 and 3.3), the protocol (section 3.4) and the elastic frequencies (section 3.5); the reader is referred to Fig. 10 for remarks on the associated P_f.

3.1. General results

Considering FM set (Fig. 9), the reliability associated with DS1 and DS2 is almost identical for all models, whereas some differences were found between DS3 and DS1/DS2, corresponding to models M3 and M4, and very minor differences were identified considering models M1 and M2. In particular, for models M3, DS3 reliability is higher than DS1/DS2 one for all protocols but FEMA 461, and for models M4, an opposite trend is found for all protocols. The reliability associated with DS4 and DS5 is often lower than the one related to DS1 to DS3, even though there are some cases in which an opposite trend can be observed. For models M1, DS4 (DS5) reliability is lower (significantly lower) than DS3 one for all protocols, and the smallest influence is associated with IEEE 693 protocol. Regarding M2, DS4 (DS5) reliability is lower than DS1/DS2/DS3 for FEMA 461 and is more similar to DS1/DS2/DS3 ones for other protocols (AC156w/o reliability related to DS4 is slightly lower than DS1/DS2/DS3); a completely different trend is found regarding DS5 and M2: all protocols but IEEE 693 and FEMA 461 are associated with lower reliability, if compared with other DSs.

For all protocols but FEMA 461 the reliability associated with models M3 increases passing from DS3 to DS4 and from DS4 to DS5, especially for AC156 (clear and gradual increase); for FEMA 461, negligible differences are observed passing from DS3 to DS4 and minor reliability decreases are found passing from DS4 to DS5. Reliabilities associated with models M4 are more irregular. For AC156, DS4 (DS5) reliability is extremely lower (significantly lower) than DS3 one, and a similar trend, but with overall lower reliability ranges, is found regarding AC156w/o and Zito et al. An opposite (specular) trend is found for FEMA 461 and IEEE 693 protocols, where extremely larger reliability indexes are found for DS4 and DS5, compared to DS3 ones.

3.2. Influence of key parameters

3.2.1. Floor motion sets

The different FM set (i.e., FM, NFFM, FFFM, and SFM sets) has a minor or negligible influence on the reliability, but peculiar FM sets are overall more severe than all FM set, mostly depending on models and minorly conditioned by DSs and protocols. In particular, the least regular influence is shown for M1 models, whereas the most regular influence is shown for M2 models, as well as DS1 to DS3 responses, as expected, were found to be more reasonable, especially correlating the results to the models' frequencies. Regarding M1, FFFM are overall more severe than other FMs for DS1, corresponding to AC156 and AC156w/o, DS2, DS4, corresponding to AC156, and DS5, corresponding to all protocols but IEEE 693. For DS3, SFM is more severe for AC156w/o, IEEE 693, and Zito et al.; regarding M1, in all other cases, the reliability is not or negligibly affected by FMs. For models M2, FFFM are more severe for all DSs but DS5, and in this latter case, SFM, FFFM, and NFFM provide similar severity considering AC156 and IEEE 693 protocol. Regarding

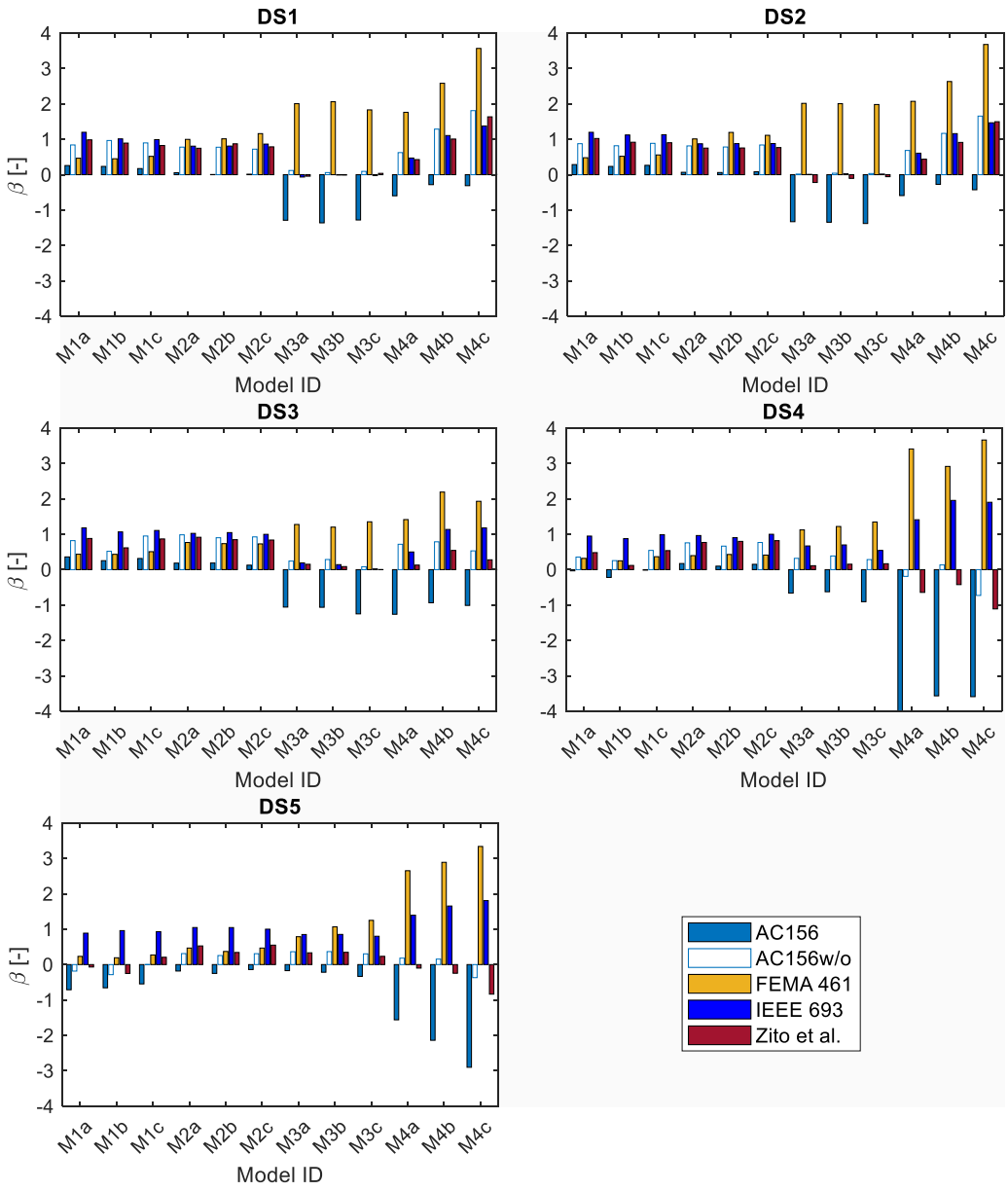

Fig. 9. Reliability index (β) associated with the investigated protocols considering floor motion (FM) set as a reference, estimated for all investigated models and damage states (DSs).

models M3, SFM are more severe for DS1, DS2, and DS3, whereas for DS4 and DS5, the severity is more comparable among the different FMs; in particular, for DS4, the different FM sets are associated with comparable severities, whereas FFFM are more severe for AC156, for both DS4 and DS5, and for AC156w/o and Zito et al., for DS5. Considering M4, SFM are more severe for DS1, DS2, and DS3, whereas no clear influence is found on severity associated with DS4, SFM are overall more severe for FEMA and IEEE 693, and FFFM are overall more severe for AC156, AC156w/o, and Zito et al.

It is recalled that M1, M2, M3, and models M4 are associated with frequencies equal to about 1.0, 1.5, 3.0, and larger than or equal to 3.0 Hz, respectively. The spectral response associated with FM sets was depicted in Fig. 2, and this response is analyzed in the light of the above mentioned evidence. In particular, it can be observed that FM sets spectral responses are relatively similar corresponding to 1.0 Hz, and this is reasonably consistent with the similar severity associated with models M1 responses. FFFM set has higher spectral response corresponding to 1.5 Hz, and this is compliant with the higher severity of this latter set of FMs regarding models M2. Similarly, SFM has the highest spectral response associated with 3.0 Hz, and this results in higher severity regarding the response of models M3. Finally, the higher spectral response related to SFM corresponding to about 6.0 Hz does not majorly influence the reliability associated with M4a model, but SFM is overall more severe for models M4 if compared to the other FM sets, especially for DS1 to DS3.

3.2.2. *Model frequency range*

The model frequency range has a major influence on the reliability of the different protocols. Models M1 and M2, corresponding to elastic frequency equal to 1.0 and 1.5 Hz, show relatively similar reliability indexes, which range within 0 – 1 for all protocols over DS1 to DS4; only for models M1, corresponding to DS4, AC156 reliability index is just lower than zero, and in these cases, this response does not represent an anomaly since AC156 reliability is slightly larger than zero in the other cases, and this means that DS4 reliability is slightly lower than DS1 to DS3 ones. Ranges 1 and 2 reliabilities related to DS5 are overall smaller

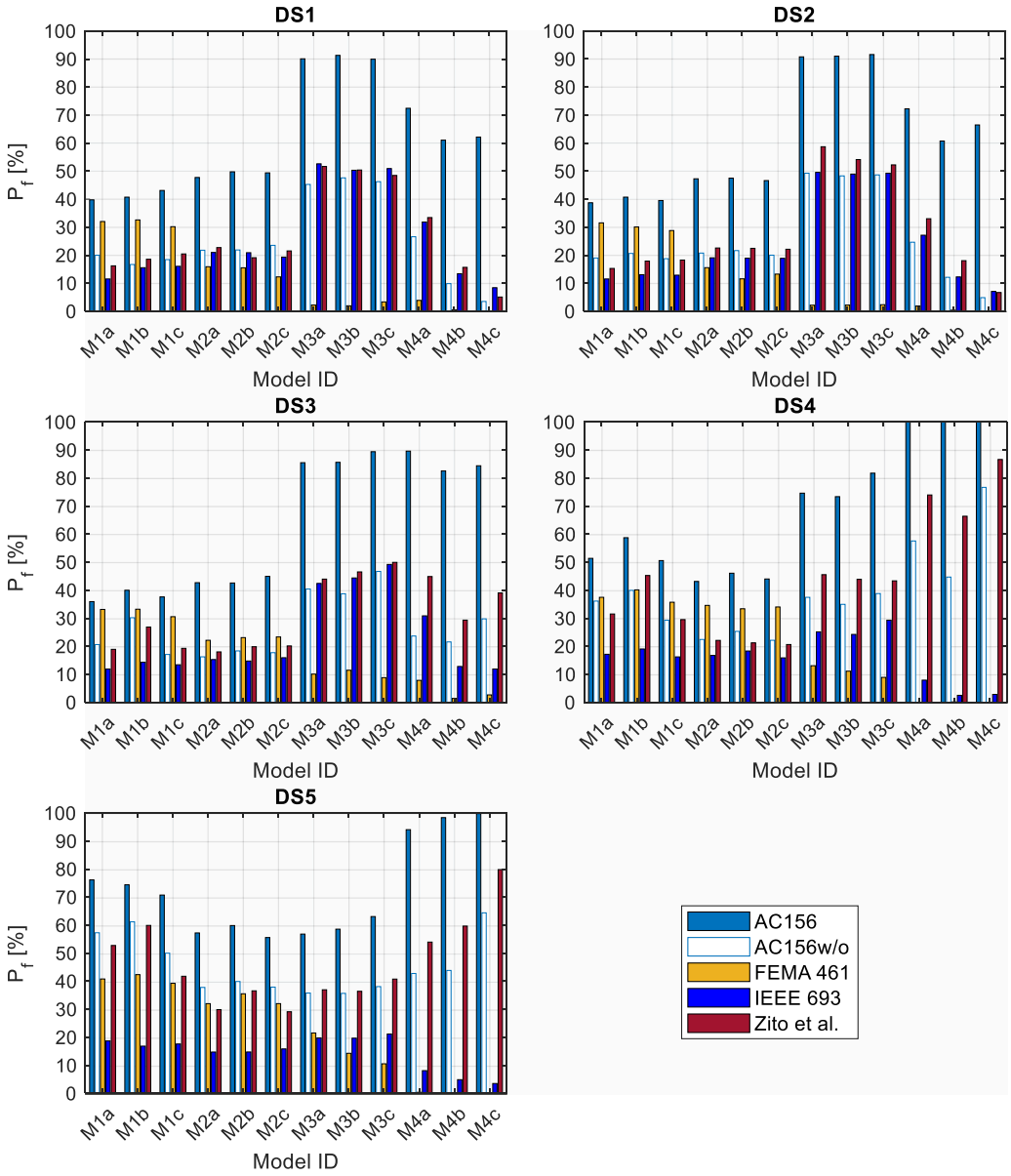

Fig. 10. Failure probability (P_f) associated with the investigated protocols considering floor motion (FM) set as a reference, estimated for all investigated models and damage states (DSs).

than the ones associated with other DSs for all protocols but IEEE 693, which exhibits reliability indexes quite similar to the ones related to other DSs. Considering DS1 to DS3, models M3, which correspond to frequencies equal to about 3.0 Hz, show a qualitatively specular reliability for AC156, corresponding to a very small reliability, i.e., β is lower than -1; considering FEMA 461 a very large reliability is observed, i.e., β is larger than 1; a relatively small reliability index is found considering other protocols (β is just smaller or larger than zero). For DS4, the specular response is still observed considering AC156 and other protocols, even though AC156 reliability indexes slightly increase; for FEMA 461, DS4 indexes are very similar to DS3.

DS5 reliability indexes related to models M3 are quite similar to the reliability indexes related to: (a) DS5 and models M2, except for FEMA 461 reliabilities that are larger for models M3, and for IEEE 693, for which the reliabilities are smaller for models M3; (b) DS4 and models M3, except for AC156 reliabilities that are smaller for DS4. Reliabilities associated with models M4 are more irregular. For AC156, DS4 and DS5 reliability are extremely lower and significantly lower than DS3 one, respectively, and a similar trend, but with overall lower reliability ranges, is found regarding AC156w/o and Zito et al. An opposite trend, which is specular, is found for FEMA 461 and IEEE 693 protocols, where extremely larger reliability indexes are found for DS4 and DS5, compared to DS3 ones.

3.2.3. *Models within model frequency range*

For DS1 to DS5 and all models but M4, there is a minor or negligible reliability dispersion within the same frequency ranges: the different models corresponding to the same frequencies are associated with reliability indexes that are almost constant within the range. A different trend is observed for models M4, as it is expected due to their different frequency. In particular, for DS1 and DS2 the reliability increases as the frequency grows for all protocols but AC156, and, in this latter case, an increase is found passing from model M4a to M4b, whereas reliability of model M4c is slightly lower than M4b one. Considering DS4, an increase in reliability is associated with growing frequency from 5 to 7 Hz for all protocols but FEMA 461, corresponding to which an opposite trend is found; these latter frequencies correspond to models M4a and M4b, respectively. Passing from 7 to 9 Hz, a reduced decrease in reliability is

observed for all protocols but FEMA 461, corresponding to which an opposite trend is found; the latter frequency range is associated with models M4b to M4c. Considering DS5, the reliability increases as the frequency grows for protocols FEMA 461 and IEEE 683, whereas it as the frequency grows for protocols AC156, AC156w/o, and Zito et al.

3.2.4. Protocol

Considering FM set as a reference, AC156 protocol is the least reliable protocol. AC156 produces negative reliability indexes for (a) all DSs for models M3 and M4, (b) DS4 for models M1, and (c) DS5 for Models M1 and M2. In all other cases, reliability of AC156 is quite scarce, with β lower and significantly lower than 0.4 (β is often similar to zero). Accordingly, this protocol does seem to be unsatisfactory and is likely to produce unsafe estimations. The enhanced version of AC156, which corresponds to AC156w/o, is more consistent with the other protocols and shows a major improvement in terms of reliability, compared with AC156. Considering DS1 to DS3 and models M1 and M2, AC156w/o, Zito et al., and IEEE 693 produce comparable reliability indexes, which are just about the unity of slightly lower; in these cases, FEMA 461 protocol shows a reliability that is lower than AC156w/o, Zito et al., and IEEE 693 protocols for models M1, whereas the abovementioned protocols is associated with a reliability that is larger than or more similar to AC156w/o, Zito et al., and IEEE 693 protocols, considering models M2.

For DS1 to DS3 and models M3, FEMA 461 reliability is significantly larger than other protocols, and AC156w/o, Zito et al., and IEEE 693 (AC156) protocols are associated with reliability indexes equal to about zero (lower than −1). Considering DS1 to DS3 and models M4, FEMA 461 reliability is the largest, and AC156w/o, Zito et al., and IEEE 693 reliability is positive; the related values are strongly depending on the model and DS.

Considering DS4 and DS5 and models M1 and M2, IEEE 693 protocol is overall the most reliable one (β equal to about the unity), whereas AC156 is the least reliable, as it was already mentioned. The reliability strongly depends on the frequency range for the other protocols, and β is overall larger for models M2 and for DS4, whereas the reliability is overall smaller for models M1 and DS5; in particular, for models M1 and DS5, AC156w/o and Zito et al. are associated with slightly negative values of β. For models M3 and M4, and DS4 and DS5, AC156 and Zito et al. reliabilities are qualitatively specular with IEEE 693 (β ranging in 1.5 – 2) and FEMA 461 (β ranging in 2.5 – 4), even though β associated with Zito et al. (β ranging in −1 to 0) is significantly larger than AC156 one (β ranging in −4 to −1.5), and relatively comparable with AC156w/o (β ranging in −1 to 0.5).

3.3. Reliability to elastic frequency correlations

The remarks qualitatively discussed in the previous sections, regarding the single model results, are quantitatively specified in this section, with regard to the correlations between β and f_a, which are depicted in Fig. 11.

The minimum β envelope of the investigated FM sets is considered as a reference for correlating β to the elastic frequency f_a, where this is meant as the minimum β selected among the four FM set responses. This errs to the side of caution and removes dependence on the FM sets, which is relatively minor. The fitting curves are also shown, and the related equations and coefficients of determinations (R^2) are reported in the Appendix. Overall, β is very well correlated with f_a through III-degree polynomial equations, even considering the inelastic DSs, resulting in almost all cases in relatively high R^2; mean, standard deviation, and coefficient of variation or R^2 set result in 0.885, 0.114, and 0.129, respectively. In particular, (a) in one case (AC156w/o and DS5) R^2 is lower than 0.600 (i.e., 0.592), (b) in three cases (AC156w/o and DS3, AC156w/o and DS4, and Zito et al. and DS5) R^2 is within 0.600 – 0.700, and in all other cases, R^2 is larger, with value often larger than 0.900 (in 17 cases out of 25). Considering all DSs, all protocol curves have relatively comparable β (−0.5 to 1) within 1 – 1.5 Hz, whereas an extremely large difference is associated with larger frequencies, especially corresponding to 6 – 9 Hz.

The major influence of DSs is stressed in Fig. 11. Considering the elastic DSs (DS1 and DS2), FEMA 461 curves have a monotonic trend,

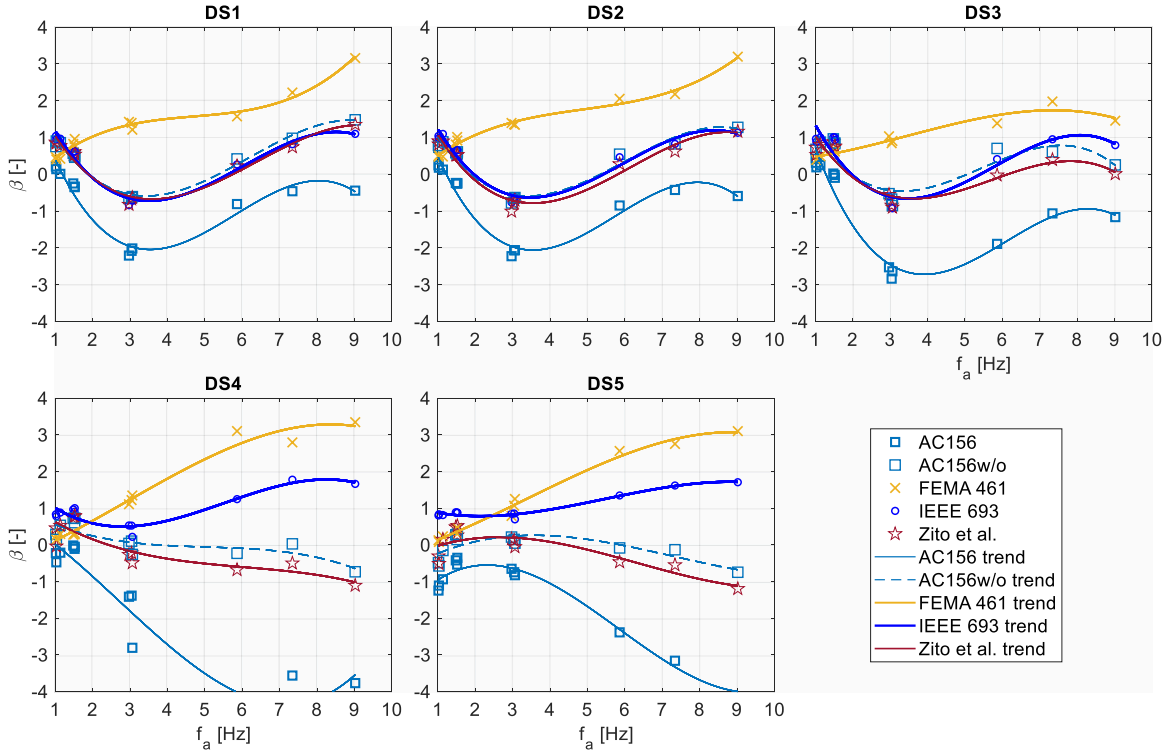

Fig. 11. Reliability index (β) corresponding to the minimum β envelope of the investigated floor motion (FM) sets, associated with the elastic frequency (f_a) of the investigated models (markers) and fitting curves (III-degree polynomial equations), estimated for all protocols and damage states (DSs).

whereas the other protocols exhibit a clear nonmonotonic tendency; in particular, as it was already highlighted in section 3.4, FEMA 461 and AC156 are associated with the highest and lowest) β, respectively, except for 1 −1.3 Hz, corresponding to which IEEE 693, AC156w/o, and Zito et al. curves have a slightly higher β. FEMA 461 curve is always associated with positive β, IEEE 693, AC156w/o, and Zito et al. curves have negative β within 1.9–5.7 Hz, and AC156 curve has negative β for frequencies higher than 1.2 Hz. IEEE 693, AC156w/o, and Zito et al. curves exhibit a very similar same trend. All protocols but FEMA 461 show their relative peaks corresponding to very similar frequencies (relative minimum point at about 3.5 Hz and maximum relative peak at about 8–9 Hz).

For DS3, FEMA 461 curve has a nonmonotonic trend, only showing a relative peak (maximum); however, the curve it is significantly flatter than other protocols, whereas the other protocols have fitting curves quite similar to DS1 and DS2, with Zito et al. curve having relative maximum peak lower than other IEEE 693 and AC156w/o. The frequency range in which IEEE 693, AC156w/o, and Zito et al. curves have β larger than FEMA 461 is quite similar to the one related to DS1 and DS2. Similarly, to DS1 and DS2, the relative peaks of all protocols but FEMA 461 correspond to very similar frequencies, which are comparable with DS1 and DS2 ones.

For DS4 and DS5, the protocol curves are more dispersed, and the trends of the curves are less comparable than for DS1 to DS3. FEMA 461 and IEEE 693 always have positive β, whereas Zito et al. and AC156w/o have positive β corresponding to 1.0–2.4 and 1.0–3.6 (1.0–4.4 and 1.7–5.8) Hz for DS4 (DS5), respectively. AC156 always has negative β for all frequencies. Considering DS4 and DS5, FEMA 461 curve has a trend similar to the one related to DS3 but the magnitude of the variation associated with DS4/DS5 is larger than DS3 one. IEEE 693 curve has β higher than AC156w/o and Zito et al., and these latter have similar trend. AC156w/o and Zito et al. curves exhibit a flatter trend (if compared to other protocols ones), which is (a) decreasing as f_a grows for DS4, (b) increasing for f_a lower than about 3–3.5 Hz for DS5, and (c) decreasing for f_a larger than about 3–3.5 Hz for DS5. Considering DS4, AC156 curve has a trend that is quite different from the one related to DS1 to DS3; in particular, only a relative peak is exhibited within the frequency range of interest for DS4 (minimum relative point corresponding to f_a equal to about 7.2 Hz). Moreover, the trend of AC156 curve associated with DS5 is relatively specular to the one associated with DS1 to DS3 response, and this is more comparable to Zito et al. and AC156w/o tendencies, even though these latter curves are significantly more flattened that AC156 one.

4. Reliability-targeted safety factors

Fig. 12 depicts the safety factor (k) corresponding to the maximum k envelope of the investigated FM sets, associated with the elastic frequency of the investigated models; k is shown as a function of each model ID (histogram) in the Appendix for the sake of completeness. The maximum k envelope is meant as the maximum k selected among the four FM set responses (side of caution and no dependency on FM sets). The k fitting curves follow III-degree polynomial equations, as β ones, and have high R^2 in many cases. Considering the entire R^2 set, mean, standard deviation, and coefficient of variation are equal to 0.744, 0.261, and 0.351, respectively. Since the coefficient of variation is just above a typical acceptable value in civil engineering applications (e.g., equal to 0.30 [72]), R^2 set is statistically assessed for fixed DSs. In particular, it is found that DS3 and DS4 are associated with relatively small mean (0.476 and 0.552, respectively), large standard deviation (0.278 and 0.233, respectively), and large coefficient of determination (0.585 and 0.423, respectively). Conversely, DS1, DS2, and DS5 are associated with significantly larger mean values (0.935, 0.896, and 0.863, respectively), significantly smaller standard deviation (0.042, 0.039, and 0.096, respectively) and significantly smaller coefficient of variation (0.045, 0.043, and 0.111, respectively). The evidence shows that the provided correlations can be quite efficient in most cases, and the cases that are not associated with acceptable correlations are clearly identified (see the Appendix). The developed correlations represent applicative abaci for estimating minimum k values as a function of the

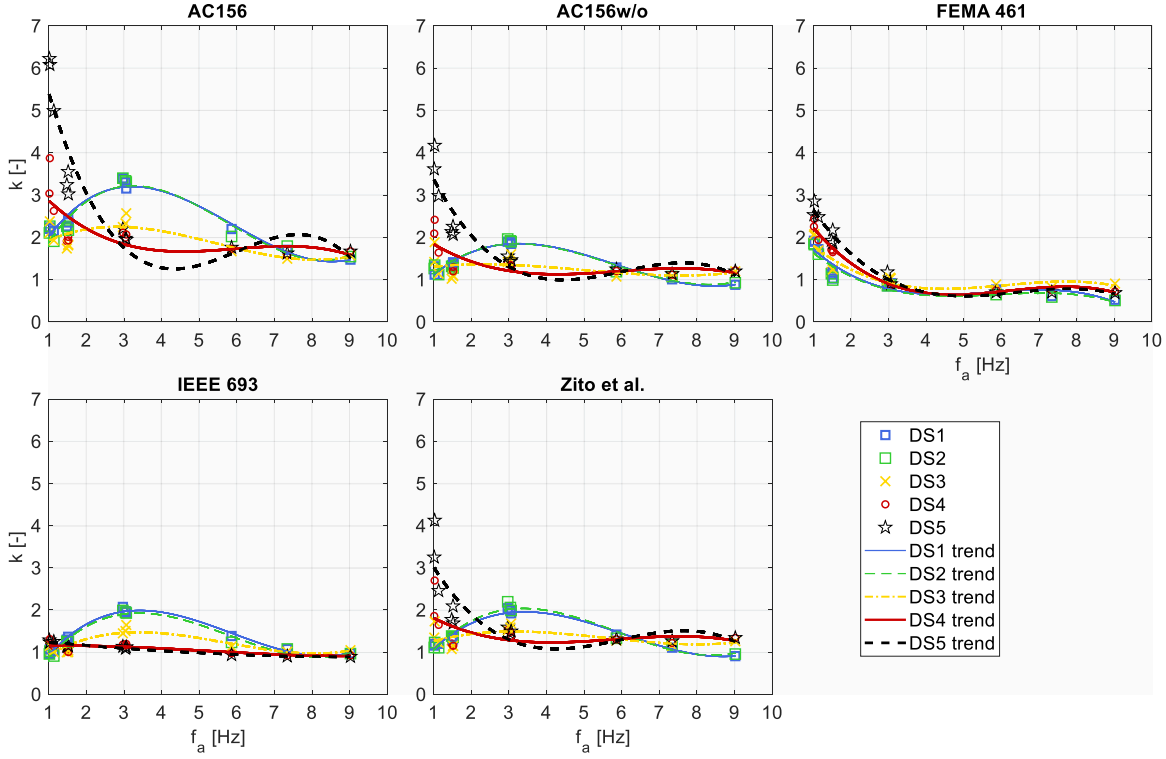

Fig. 12. Safety factor (k) corresponding to the maximum k envelope of the investigated floor motion (FM) sets, associated with the elastic frequency (f_a) of the investigated models (markers) and fitting curves (III-degree polynomial equations), estimated for all damage states (DSs) and protocols.

protocol, DSs, and elastic frequencies, and, with due consideration, the can be usefully and robustly implemented in the practice.

k versus f_a curves for DS1 and DS2 related to all protocols but FEMA 461 have the same qualitative behavior, i.e., relative maximum (minimum) point corresponding to about 3.0 – 3.5 (8 − 9) Hz and inflexion point between 5.9 and 7.3 Hz, with different k peak values; the relative maximum k values are equal to about 3.2, 1.8, 2.0, 2.0 for AC156, AC156w/o, IEEE 693, and Zito et al., respectively. FEMA 461 protocol shows very similar curves among the different DSs, and the trend is overall decreasing from 1 to 4 Hz, slightly increasing from 4 to about 7.5 – 8 Hz. In particular, the absolute maxima correspond to 1.0 Hz, and the maximum k value related to DS1 and DS2 is equal to about 2.0.

DS3 trends are similar to DS1 and DS2, but overall, the fitting curves are flatter than DS1 and DS2 ones, with maximum and inflexion point frequencies similar to the ones associated with DS1 and DS2. The relative maximum k values associated with AC156, AC156w/o, IEEE 693, and Zito et al. corresponds to 2.3, 1.4, 1.5, and 1.5, respectively, whereas for FEMA 461 the absolute maximum point corresponds to a k value equal to 1.0.

For given protocols, DS4 and DS5 curves have a similar trend even though the k values are significantly different among the different DSs, including FEMA 461 protocol. In particular, the fitting curves related to all protocols but IEEE 693 have a relative minimum (maximum) point corresponding to about 4 – 4.5 (7.5 – 8) Hz, with the inflexion frequency comparable with the one related to other cases. DS4 and DS5 curves related to IEEE 693 are significantly flatter than other ones, with a trend that is essentially slightly decreasing. All DS4 and DS5 curves present maximum absolute value corresponding to 1.0 Hz, and all protocols but FEMA 461 and IEEE 693 present a large discrepancy between the maximum values related to DS4 and DS5. In particular, the absolute maximum k values related to DS4 (DS5) are equal to 2.9, 1.9, 2.2, 1.2, and 1.9 (5.4, 3.3, 2.7, 1.2, and 3) corresponding to AC156, AC156w/o, FEMA 461, IEEE 693, and Zito et al., respectively. The relative maximum k values associated with DS4 (DS5) are equal to 1.8, 1.2, 0.8, 1, and 1.4 (2.1, 1.4, 0.8, 0.9, and 1.5), respectively.

Despite AC156 protocol was found to be significantly more unreliable than other protocols for all DSs and models, the AC156 k values are not significantly larger than the other protocols, especially for frequencies larger than 1 Hz and for FEMA 461 results. This can be explained by recalling that k increases as the dispersion associated with the protocol grows, as it can be seen in Eq. (8) and in Fig. 8. In particular, AC156 protocol is associated with a relatively low dispersion, if compared with other protocols, with particular regard to FEMA 461. An emblematic case was depicted in Fig. 8: even though point A condition is associated with a reliability index significantly lower than point C condition, k related to A is lower than the one associated with C, and this is due to the larger dispersion associated with C results. It should be recalled that FEMA 461 set consists in only three records, whereas other protocols have more records (i.e., AC156, AC156w/o, and Zito et al. include seven records and IEEE 693 consists in ten signals); the motivation for only considering three FEMA 461 signals were discussed in [35]. Further comments are omitted for the sake of brevity, and the technical recommendations associated with Fig. 12 are reported in the following section.

5. Technical recommendations and concluding remarks

The study developed novel knowledge in the field of seismic assessment of NEs, with regard to both methodology and findings. The methodology is generally applicable to seismic capacity generation procedures and tools, also different from shake table testing, and case studies also different from inelastic SDOF NEs. The following technical recommendations and concluding remarks can be derived in the light of the reported evidence.

- Considering serviceability conditions and elastic response, the seismic response of NEs having low fundamental frequencies, e.g., lower than 3 – 4 Hz, might be relatively critical for all protocols, if compared with NEs having larger fundamental frequencies.
- Very low frequencies might be extremely critical for the assessment of ultimate conditions and inelastic response, and particular attention should be focused on these latter cases. The general criticality of the protocols regarding lower frequencies might be associated with the relatively lower frequency contents associated with these frequencies, and this result is in relatively good agreement with the findings reported in [35,39], even though these latter studies focused on rocking-dominated elements.
- AC156 protocol is not recommended to be used to assess performance levels associated with ultimate conditions, as well as it is not found to be optimal for assessing service conditions. In these latter conditions, AC156 might be used but relatively large safety factors should be considered. This evidence represents a breakthrough since the latter protocol was widely used in the practice and is still among the most used ones for assessment and qualification purposes, as it was discussed in the Introduction.
- IEEE 693 protocol seems to be the safest protocol for the assessment of ultimate conditions, and it is found to be stable with regard to the fundamental frequencies. The other protocols but AC156 might be used by considering larger safety factors, and particular attention should be focused on very low frequencies for AC156w/o and Zito et al. protocols.
- All protocols (but AC156) could be used when the serviceability performance is investigated, and the variation of the safety factor is relatively reduced over the different protocols and frequencies. Particular attention should be focused on frequencies in the vicinity of 3 (1) Hz considering AC156w/o, IEEE 693, and Zito et al. (FEMA 461).
- The fit curves reported in the previous section correlate k to the fundamental frequencies for all protocols and DSs. These curves could be used as applicative abaci for estimating reliable and robust safety factors (minimum values) for seismic assessment of NEs that can be modeled by inelastic SDOF, with regard to both serviceability and ultimate limit conditions of NEs. In particular, the seismic capacity assessed by means of shake table testing, using the protocol of interest, could be divided by the provided k values in order to enforce a reliability-targeted capacity estimation, considering representative FMs as a reference.
- The provided correlations are associated with a relatively reasonable target reliability index, equal to one, but the methodology could be extended to other target values, in order to account for higher or lower target reliability.

The study develops a robust means for seismic assessment of NEs by means of shake table testing, in terms of both methodology, findings, and technical recommendations. The methodology completely revolutionizes the assessment approach and the reliability evaluation since it allows the estimation of reliability indexes and safety factors towards a reliability-targeted seismic assessment and qualification of NEs. The reliability of the investigated protocols, the associated safety factors, and the technical recommendations can be referred to for NEs that are compatible with the ones investigated in this study, i.e., inelastic SDOF elements. In particular, the findings are not meant to be extendable to NEs that are governed by rigid motions, such as rocking- and sliding-dominated elements. Further studies should investigate other NE case studies and should experimentally validate the present study.

CRediT authorship contribution statement

Zito Martino: Data curation, Software, Visualization. **Di Salvatore Chiara:** Data curation, Investigation, Methodology, Software. **Magliulo Gennaro:** Conceptualization, Formal analysis, Funding acquisition,

Methodology, Project administration, Resources, Supervision, Validation, Writing – review & editing. **D'Angela Danilo:** Conceptualization, Data curation, Investigation, Methodology, Validation, Writing – original draft, Writing – review & editing.

Declaration of Competing Interest

The authors declare that they have no known competing financial interests or personal relationships that could have appeared to influence the work reported in this paper.

Data Availability

Data will be made available on request.

Acknowledgements

The study was funded by (1) the Italian Ministry of University and Research (MUR) in the framework of PRIN 2020 project titled "ENRICH project: ENhancing the Resilience of Italian healthCare and Hospital facilities" and by (2) the National project DPC – ReLUIS 2022–2024 WP17: "Code contributions for nonstructural elements" (Italian Department of Civil Protection (DPC)). The technical support of Giuseppe Toscano for the numerical implementation and analytical work is fully acknowledged, as well as Valentina Santaniello is thanked for data curation and elaboration.

Appendix

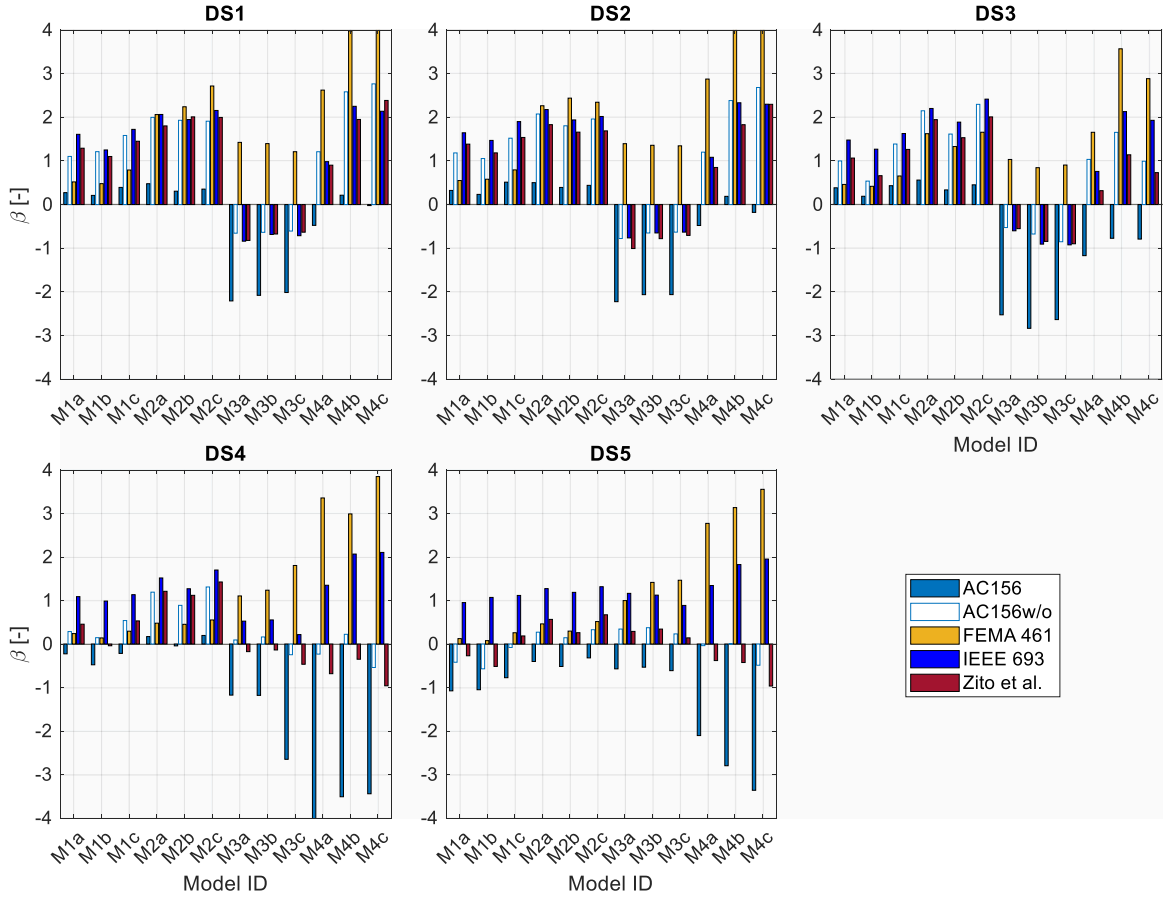

Fig A1. Reliability index (β) associated with the investigated protocols considering strong floor motion (SFM) set as a reference, estimated for all investigated models and damage states (DSs).

.

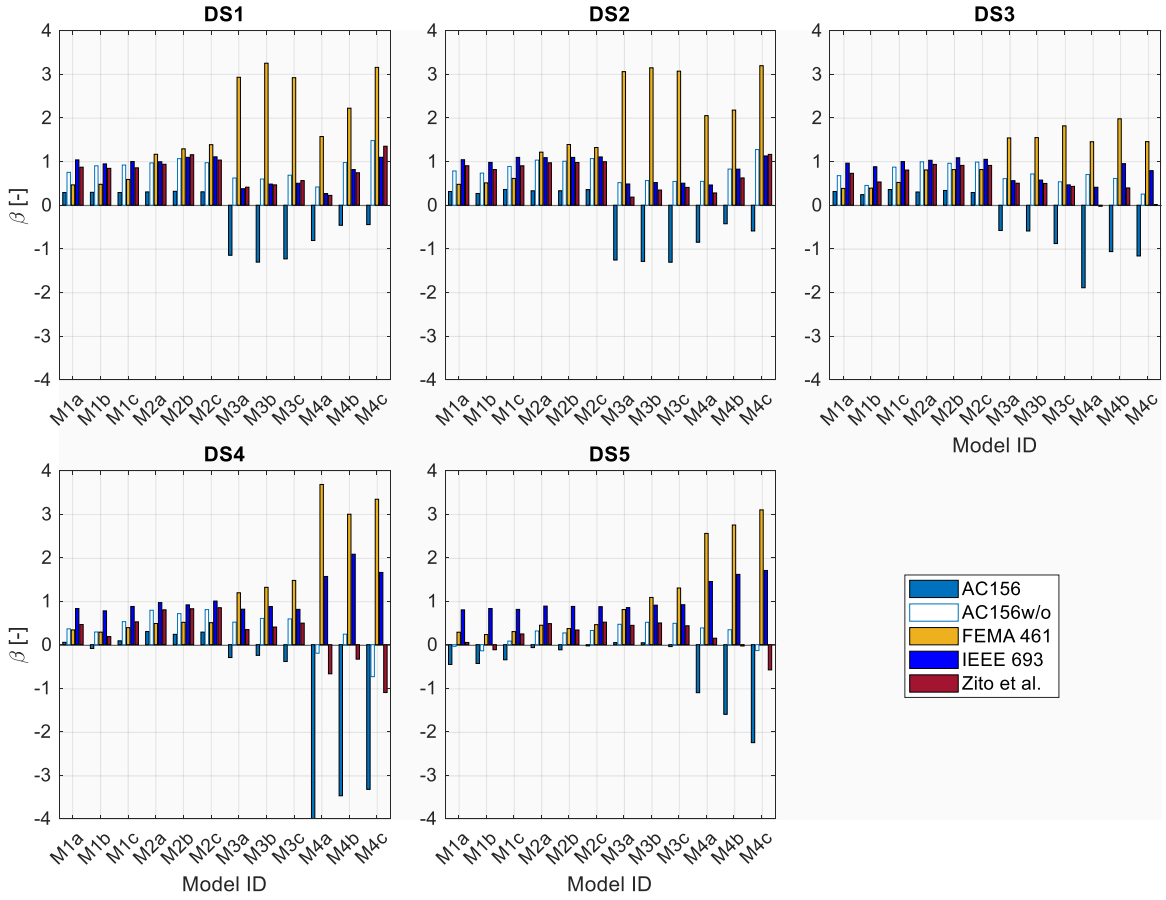

Fig A2. Reliability index (β) associated with the investigated protocols considering near field floor motion (NFFM) set as a reference, estimated for all investigated models and damage states (DSs).

.

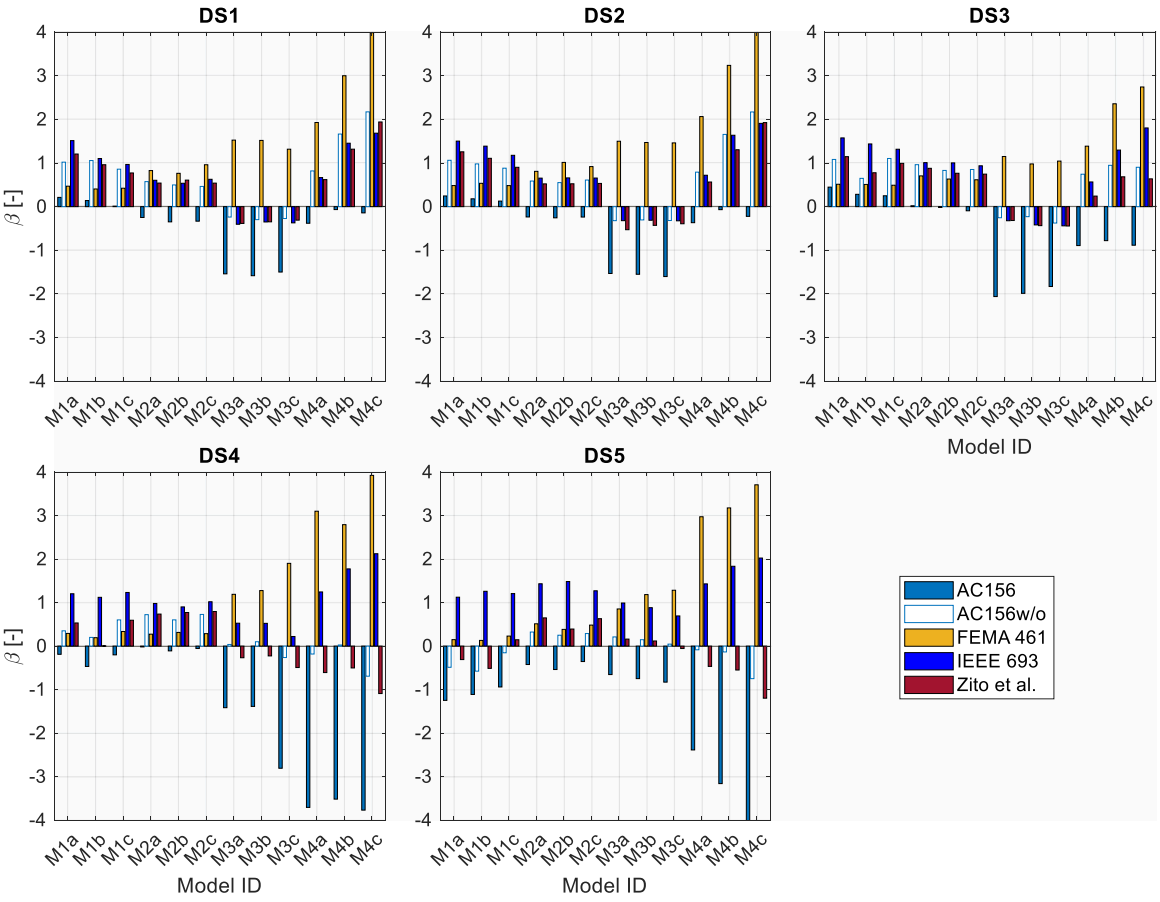

Fig A3. Reliability index (β) associated with the investigated protocols considering far field floor motion (FFFM) set as a reference, estimated for all investigated models and damage states (DSs).

.

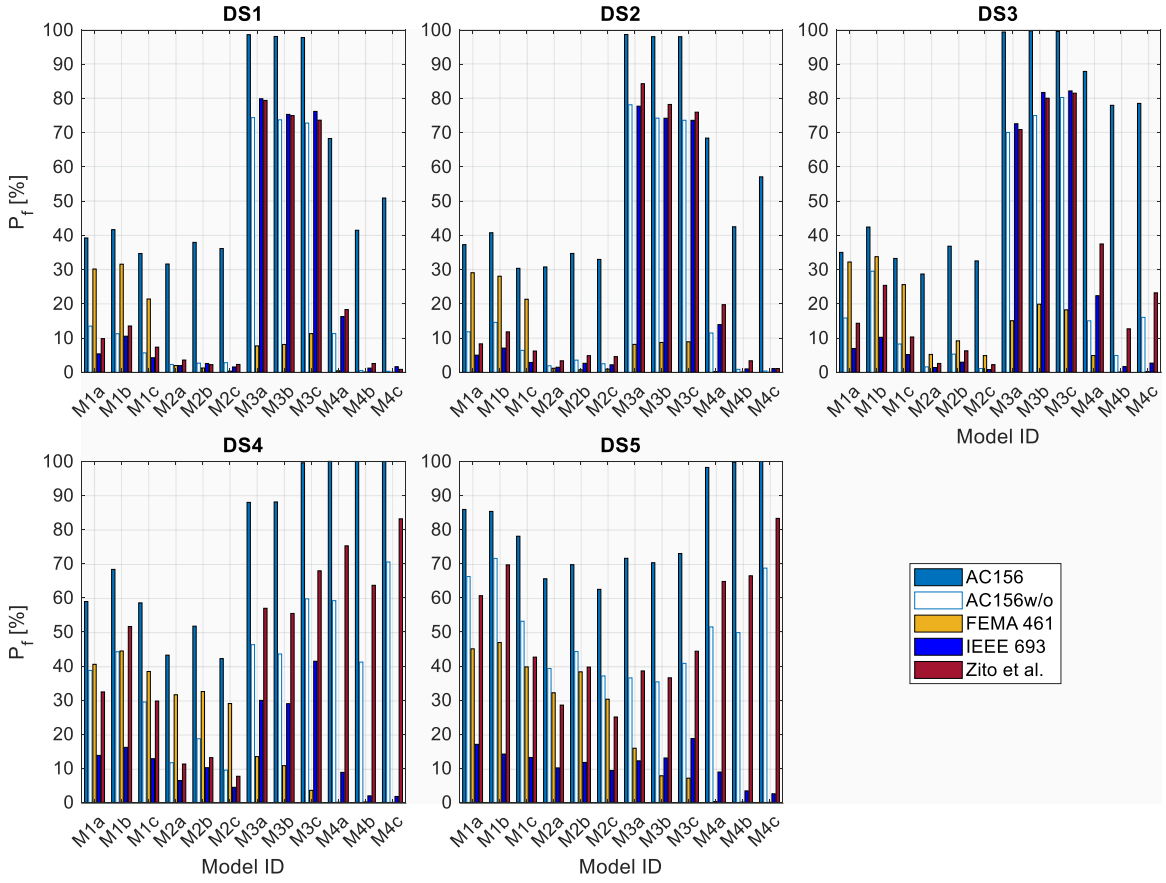

Fig A5. Failure probability (P_f) associated with the investigated protocols considering strong floor motion (SFM) set as a reference, estimated for all investigated models and damage states (DSs).

.

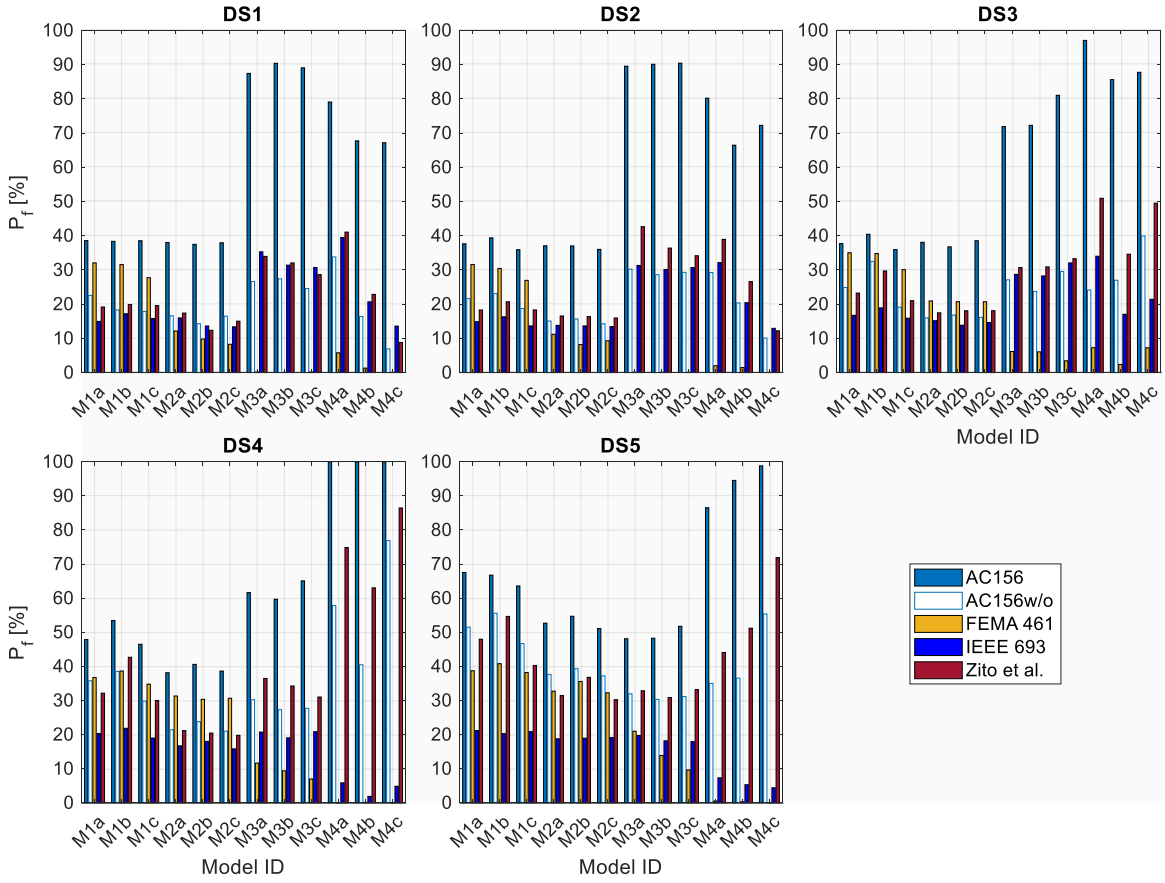

Fig A6. Failure probability (P_f) associated with the investigated protocols considering near field floor motion (NFFM) set as a reference, estimated for all investigated models and damage states (DSs).

.

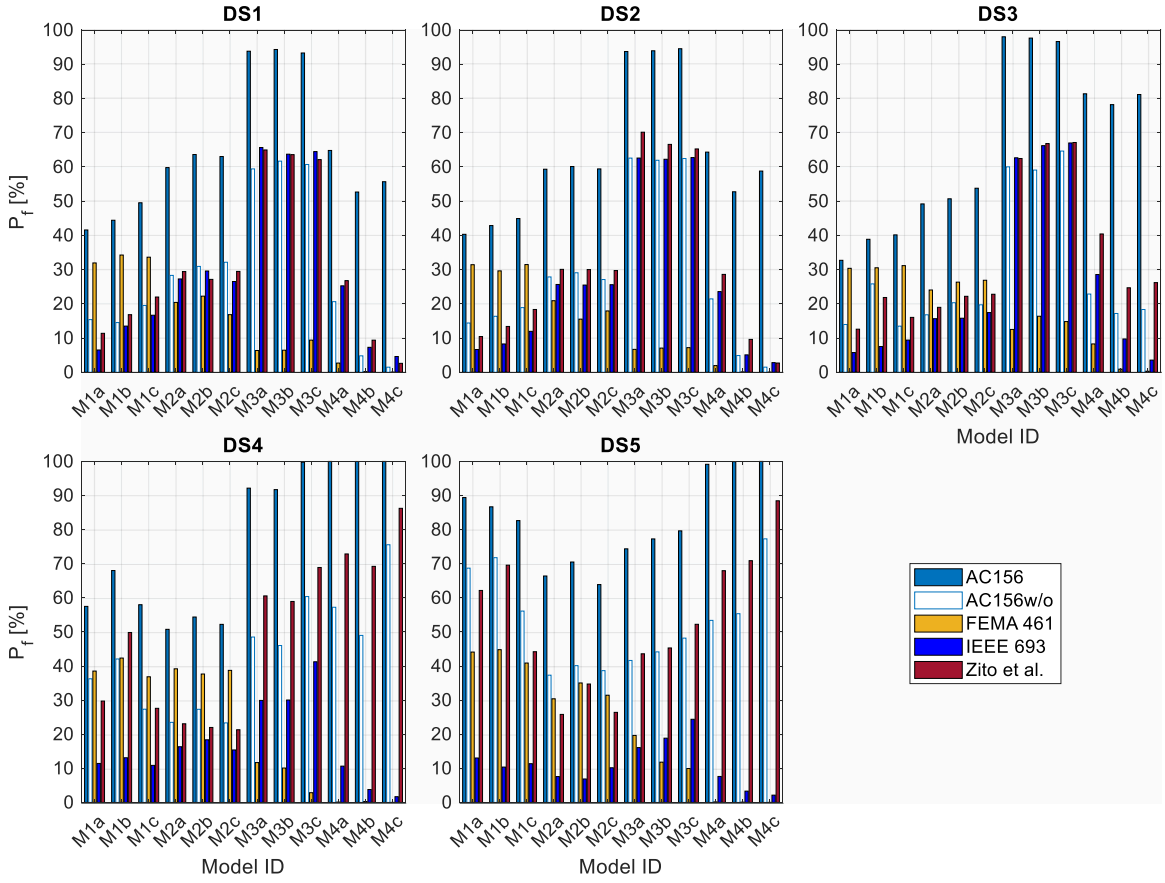

Fig A7. Failure probability (P_f) associated with the investigated protocols considering far field floor motion (FFFM) set as a reference, estimated for all investigated models and damage states (DSs).

.

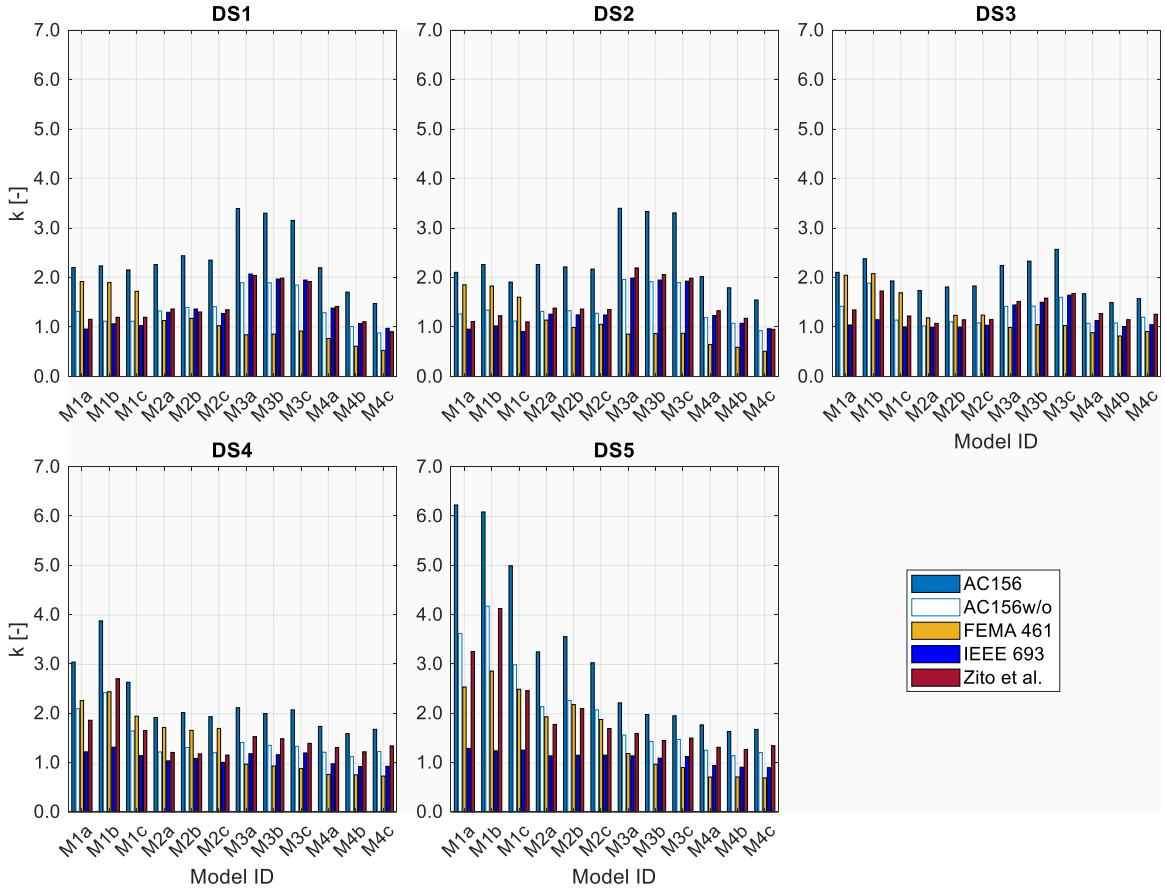

Fig A8. Safety factor (k) associated with the maximum k envelope of the investigated floor motion (FM) sets, estimated for all investigated models and damage states (DSs).

Table A1

Reliability index (β) versus elastic frequency (f_a): fitting equations ($\beta = af_a^3 + bf_a^2 + cf_a + d$) and coefficient of determinations (R^2). The equations associated with R^2 lower than 0.65 are reported in bold font.

(a;b;c;d) R^2 [-]	DS1	DS2	DS3	DS4	DS5
AC156	(−0.0408;0.709;−3.49;3.22) 0.949	(−0.0431;0.743;−3.64;3.42) 0.948	(−0.0428;0.783;−4.16;4.14) 0.930	(0.0156;−0.125;−0.614;0.738) 0.905	(0.0199;−0.348;1.29;−1.92) 0.973
AC156w/o	(−0.0254;0.469;−2.33;2.89) 0.967	(−0.0271;0.488;−2.38;2.94) 0.917	(−0.0325;0.53;−2.44;2.99) 0.685	(−0.00736;0.111;−0.593;1.04) 0.669	**(0.00546;−0.12;0.646;−0.77) 0.592**
FEMA 461	(0.0158;−0.223;1.14;−0.484) 0.983	(0.0119;−0.175;0.997;−0.325) 0.986	(−0.00588;0.0614;0.0534;0.369) 0.933	(−0.00648;0.0562;0.418;−0.352) 0.977	(−0.00556;0.0563;0.309;−0.218) 0.987
IEEE 693	(−0.03;0.541;−2.69;3.36) 0.967	(−0.0307;0.547;−2.69;3.41) 0.951	(−0.0351;0.608;−2.95;3.72) 0.838	(−0.0158;0.262;−1.09;1.85) 0.864	(−0.00631;0.104;−0.355;1.13) 0.966
Zito et al.	(−0.0234;0.447;−2.3;2.91) 0.955	(−0.0277;0.51;−2.57;3.16) 0.940	(−0.0277;0.475;−2.35;2.95) 0.798	(−0.00611;0.111;−0.761;1.28) 0.756	(0.00698;−0.132;0.55;−0.454) 0.702

Table A2

Safety factor (k) versus elastic frequency (f_a): fitting equations ($k = af_a^3 + bf_a^2 + cf_a + d$) and coefficient of determinations (R^2). The equations associated with R^2 lower than 0.65 are reported in bold font.

(a;b;c;d) R^2 [-]	DS1	DS2	DS3	DS4	DS5
AC156	(0.0237;−0.417;1.95;0.462) 0.938	(0.0271;−0.469;2.19;0.13) 0.879	**(0.0104;−0.17;0.707;1.37) 0.528**	**(−0.0123;0.219;−1.23;3.9) 0.542**	(−0.0453;0.812;−4.49;9.13) 0.879
AC156w/o	(0.0143;−0.252;1.19;0.164) 0.949	(0.0147;−0.255;1.19;0.175) 0.870	**(0.00371;−0.0549;0.195;1.16) 0.111**	**(−0.00806;0.143;−0.782;2.49) 0.466**	(−0.0246;0.445;−2.5;5.45) 0.848
FEMA 461	(−0.0124;0.213;−1.16;2.67) 0.855	(−0.0103;0.182;−1.03;2.49) 0.849	(−0.01;0.184;−1.05;2.68) 0.802	(−0.0138;0.258;−1.51;3.49) 0.974	(−0.0154;0.296;−1.81;4.17) 0.974

(*continued on next page*)

Table A2 (*continued*)

(a;b;c;d) R^2 [-]	DS1	DS2	DS3	DS4	DS5
IEEE 693	(0.0184;−0.324;1.57;−0.335) 0.976	(0.0192;−0.333;1.6;−0.408) 0.954	(0.00981;−0.169;0.808;0.29) 0.738	**(0.00127;−0.0198;0.0524;1.11) 0.523**	(0.000197;0.00156;−0.0757;1.3) 0.923
Zito et al.	(0.0144;−0.262;1.29;0.0379) 0.957	(0.0176;−0.311;1.5;−0.16) 0.928	**(0.00519;−0.087;0.393;0.95) 0.200**	**(−0.00727;0.127;−0.675;2.36) 0.257**	(−0.0219;0.392;−2.14;4.79) 0.690

References

[1] Achour N, Miyajima M, Kitaura M, Price A. Earthquake-induced structural and nonstructural damage in hospitals. Earthq Spectra 2011;27:617–34. https://doi.org/10.1193/1.3604815.

[2] Baird A, Tasligedik AS, Palermo A, Pampanin S. Seismic performance of vertical nonstructural components in the 22 february 2011 Christchurch earthquake. Earthq Spectra 2014;30:401–25. https://doi.org/10.1193/031013EQS067M.

[3] Miranda E, Mosqueda G, Retamales R, Pekcan G. Performance of nonstructural components during the 27 February 2010 Chile earthquake. Earthq Spectra 2012; 28:453–71. https://doi.org/10.1193/1.4000032.

[4] Yön B, Onat O, Öncü ME. Earthquake damage to nonstructural elements of reinforced concrete buildings during 2011 van seismic sequence. J Perform Constr Facil 2019;33:04019075. https://doi.org/10.1061/(ASCE)CF.1943-5509.0001341.

[5] Perrone D, Calvi PM, Nascimbene R, Fischer EC, Magliulo G. Seismic performance of non-structural elements during the 2016 Central Italy earthquake. Bull Earthq Eng 2019;17:5655–77. https://doi.org/10.1007/s10518-018-0361-5.

[6] Taghavi S, Miranda E. Response assessment of nonstructural building elements. PEER Report. Pac Earthq Eng Res Cent: Univ Calif Berkeley, Berkeley, Calif 2003/05:2003.

[7] O'Reilly GJ, Calvi GM. A seismic risk classification framework for non-structural elements. Bull Earthq Eng 2021;19:5471–94. https://doi.org/10.1007/s10518-021-01177-y.

[8] Magliulo G, D'Angela D, Lopez P, Manfredi G. Nonstructural seismic loss analysis of traditional and innovative partition systems housed in code-conforming RC frame buildings. J Earthq Eng 2021:1–28. https://doi.org/10.1080/13632469.2021.1983488.

[9] Federal Emergency Management Agency (FEMA). Interim protocols for determining seismic performance characteristics of structural and nonstructural components through laboratory testing. Report No. FEMA 461. Washington D.C., USA: 2007.

[10] Joyner MD, Sasani M. Building performance for earthquake resilience. Eng Struct 2020;210:110371. https://doi.org/10.1016/j.engstruct.2020.110371.

[11] American Society of Civil Engineers, editor. ASCE 7–16. Minimum design loads for buildings and other structures. Reston, Va: American Society of Civil Engineers: Structural Engineering Institute; 2017.

[12] Zito M, Nascimbene R, Dubini P, D'Angela D, Magliulo G. Experimental seismic assessment of nonstructural elements: testing protocols and novel perspectives. Buildings 2022;12:1871. https://doi.org/10.3390/buildings12111871.

[13] Shang Q, Li J, Du C, Wang T. Seismic fragility analysis of freestanding hospital cabinets based on shaking table tests. J Earthq Eng 2023;27:1993–2012. https://doi.org/10.1080/13632469.2022.2091684.

[14] Retamales R, Mosqueda G, Filiatrault A, Reinhorn A. Testing protocol for experimental seismic qualification of distributed nonstructural systems. Earthq Spectra 2011;27:835–56. https://doi.org/10.1193/1.3609868.

[15] Fiorino L, Bucciero B, Landolfo R. Evaluation of seismic dynamic behaviour of drywall partitions, façades and ceilings through shake table testing. Eng Struct 2019;180:103–23. https://doi.org/10.1016/j.engstruct.2018.11.028.

[16] Di Sarno L, Magliulo G, D'Angela D, Cosenza E. Experimental assessment of the seismic performance of hospital cabinets using shake table testing. Earthq Eng Struct Dyn 2019;48:103–23. https://doi.org/10.1002/eqe.3127.

[17] International Code Council Evaluation Service (ICC-ES). AC156 Acceptance Criteria for the Seismic Qualification of Nonstructural Components. Brea, California, USA: 2012.

[18] Wittich CE, Hutchinson TC. Rocking bodies with arbitrary interface defects: analytical development and experimental verification. Earthq Engng Struct Dyn 2018;47:69–85. https://doi.org/10.1002/eqe.2937.

[19] Ghith A, Ezzeldin M, Tait M, El-Dakhakhni W. Shake table seismic performance assessment of auxiliary battery power systems using the FEMA 461 protocol. J Struct Eng 2019;145:04019080. https://doi.org/10.1061/(ASCE)ST.1943-541X.0002341.

[20] Petrone C, Magliulo G, Manfredi G. Shake table tests for the seismic assessment of hollow brick internal partitions. Eng Struct 2014;72:203–14. https://doi.org/10.1016/j.engstruct.2014.04.044.

[21] Mosqueda G, Retamales R, Filiatrault A, Reinhorn A. Testing facility for experimental evaluation of non-structural components under full-scale floor motions. Struct Des Tall Spec Build 2009;18:387–404. https://doi.org/10.1002/tal.441.

[22] International Code Council Evaluation Service (ICC-ES). AC156 Acceptance Criteria for the Seismic Qualification of Nonstructural Components. Brea, California, USA: 2020.

[23] Institute of Electrical and Electronics Engineers. 693-2018 - IEEE Recommended Practice for Seismic Design of Substations (Revision of IEEE Std 693–2005). New York: Institute of Electrical and Electronics Engineers; 2019.

[24] Institute of Electrical and Electronics Engineers (IEEE). IEEE 344. Seismic Qualification of Equipment for Nuclear Power Generating Stations 2013.

[25] Network Infrastructure and Operations. NEBS Requirements: Physical Protection. Telcordia Technologies Generic Requirements, GR-63-CORE. 2006.

[26] Takhirov S.M., Fujisaki E., Power B., Vancouver A., Riley W.M., Low B. PEER Report No. 2017/10. Development of Time Histories for IEEE693 Testing and Analysis (Including Seismically Isolated Equipment). Berkeley (CA): Pacific Earthquake Engineering Research Center, University of California; 2017.

[27] Perrone D., Brunesi E., Decarro F., Peloso S., Filiatrault A. Seismic Assessment and Qualification of Non-structural Elements in Europe: a Critical Review. 4th International Workshop on the Seismic Performance of Non-Structural Elements (SPONSE), Pavia, Italy: 2019. https://doi.org/10.7414/4sponse.ID.10.

[28] Prota A, Zito M, D'Angela D, Toscano G, Ceraldi C, Fiorillo A, et al. Preliminary results of shake table tests of a typical museum display case containing an art object. Adv Civ Eng 2022;2022:1–18. https://doi.org/10.1155/2022/3975958.

[29] Patnana V, Rai DC. Experimental testing on nonstructural continuous plasterboard suspended ceiling systems under shake table-generated motions. Earthq Spectra 2022;38:1918–45. https://doi.org/10.1177/87552930221085298.

[30] Zhou H, Shao X, Tian Y, Xu G, Shang Q, Li H, et al. Reproducing response spectra in shaking table tests of nonstructural components. Soil Dyn Earthq Eng 2019;127: 105835. https://doi.org/10.1016/j.soildyn.2019.105835.

[31] Zito M, D'Angela D, Maddaloni G, Magliulo G. A shake table protocol for seismic assessment and qualification of acceleration-sensitive nonstructural elements. Comput Aided Civ Eng 2022:mice.12951. https://doi.org/10.1111/mice.12951.

[32] Petrone C, Magliulo G, Manfredi G. Seismic demand on light acceleration-sensitive nonstructural components in European reinforced concrete buildings. Earthq Eng Struct Dyn 2015;44:1203–17. https://doi.org/10.1002/eqe.2508.

[33] Cao Y, Qu Z, Ji X. A building-specific dynamic loading protocol for experimental tests on nonstructural elements. J Earthq Eng 2023:1–21. https://doi.org/10.1080/13632469.2023.2168798.

[34] Wittich C.E., Hutchinson T.C. Development Of A Rocking-Period Centered Protocol For Shake Table Testing Of Unattached Stiff Components. Tenth U.S. National Conference on Earthquake Engineering. Frontiers of Earthquake Engineering, Anchorage, Alaska: 2014. https://doi.org/DOI: 10.4231/D3BN9X373.

[35] D'Angela D, Magliulo G, Cosenza E. Towards a reliable seismic assessment of rocking components. Eng Struct 2021;230:111673. https://doi.org/10.1016/j.engstruct.2020.111673.

[36] D'Angela A, Magliulo G, Cosenza E. Incremental dynamic analysis of rigid blocks subjected to ground and floor motions and shake table protocol inputs. Bull NZ Soc Earthq Eng 2022;55. https://doi.org/10.5459/bnzsee.55.2.64-79.

[37] Anajafi H, Medina RA. Evaluation of ASCE 7 equations for designing acceleration-sensitive nonstructural components using data from instrumented buildings. Earthq Engng Struct Dyn 2018;47:1075–94. https://doi.org/10.1002/eqe.3006.

[38] Petrone C, Magliulo G, Manfredi G. Floor response spectra in RC frame structures designed according to Eurocode 8. Bull Earthq Eng 2016;14:747–67. https://doi.org/10.1007/s10518-015-9846-7.

[39] D'Angela D, Magliulo G, Cosenza E. Seismic damage assessment of unanchored nonstructural components taking into account the building response. Struct Saf 2021;93:102126. https://doi.org/10.1016/j.strusafe.2021.102126.

[40] CESMD. Center for Engineering Strong Motion Data 2017. ⟨www.strongmotioncenter.org⟩. Download on October 31st 2017.

[41] International Code Council. 2018 IBC code and commentary. 2018.

[42] Wilcoski J., Gambill J., Smith S. CERL equipment fragility and protection procedure (CEFAPP). USACERL Technical Rep. No. 97/58. Champaign, IL: 1997.

[43] Takhirov S.M., Fujisaki E., Power B., Vancouver A., Riley W.M., Low B. PEER Report No. 2017/10. Development of Time Histories for IEEE693 Testing and Analysis (Including Seismically Isolated Equipment). Berkeley (CA): Pacific Earthquake Engineering Research Center, University of California; 2017.

[44] Ministero delle Infrastrutture e dei Trasporti. Circolare 21. gennaio 2019. C S Ll Pp Istruzioni per l'applicazione dell'"Aggiornamento delle "Norme Tec per Le costruzioni"" di cui al Decret Minist 17 gennaio 2019;2018(n. 7).

[45] Ministero delle Infrastrutture e dei Trasporti. D.M. del 17/01/2018 – "Aggiornamento delle Norme tecniche per le Costruzioni 2018" NTC 2018 (in Italian) 2018.

[46] Chichino B, Peloso S, Bolognini D, Moroni C, Perrone D, Brunesi E. Towards seismic design of nonstructural elements: italian code-compliant acceleration floor response spectra. Adv Civ Eng 2021;2021:1–18. https://doi.org/10.1155/2021/4762110.

[47] Di Domenico M, Ricci P, Verderame GM. Floor spectra for bare and infilled reinforced concrete frames designed according to Eurocodes. Earthq Engng Struct Dyn 2021:eqe.3523. https://doi.org/10.1002/eqe.3523.
[48] Magliulo G, Pentangelo V, Maddaloni G, Capozzi V, Petrone C, Lopez P, et al. Shake table tests for seismic assessment of suspended continuous ceilings. Bull Earthq Eng 2012;10:1819–32. https://doi.org/10.1007/s10518-012-9383-6.
[49] Petrone C, Magliulo G, Manfredi G. Shake table tests on standard and innovative temporary partition walls. Earthq Eng Struct Dyn 2017;46:1599–624. https://doi.org/10.1002/eqe.2872.
[50] International Organization for Standardization. ISO 13033:2013. Bases for design of structures – Loads, forces and other actions – Seismic actions on nonstructural components for building applications 2013.
[51] U.S. Nuclear Regulatory Commission (NRC). Regulatory Guide 1.60: Design Response Spectra for Seismic Design of Nuclear Power Plants. Rockville, MD: U.S. Nuclear Regulatory Commission (NRC); 2014.
[52] International Electrotechnical Commission (IEC). IEC 60068. Environmental Testing—Part 2-57: Tests—Test Ff: Vibration—Time-history And Sine-beat Method. Geneva, Switzerland: International Electrotechnical Commission (IEC); 2019.
[53] Merino RJ, Perrone D, Filiatrault A. Consistent floor response spectra for performance-based seismic design of nonstructural elements. Earthq Engng Struct Dyn 2020;49:261–84. https://doi.org/10.1002/eqe.3236.
[54] Akkar S, Bommer JJ. Prediction of elastic displacement response spectra in Europe and the Middle East. Earthq Engng Struct Dyn 2007;36:1275–301. https://doi.org/10.1002/eqe.679.
[55] British Standards Institution, European Committee for Standardization. Eurocode 8 Design Of Structures For Earthquake Resistance 2005 British Standards Institution, London.
[56] Riley M, Stark C, Kempner L, Mueller W. Seismic retrofit using spring damper devices on high-voltage equipment stands. Earthq Spectra 2006;22:733–53. https://doi.org/10.1193/1.2216736.
[57] Gesualdo A, Iannuzzo A, Minutolo V, Monaco M. Rocking of freestanding objects: theoretical and experimental comparisons. J Theor Appl Mech 2018;56:977–91. https://doi.org/10.15632/jtam-pl.56.4.977.
[58] Papadopoulos K, Vintzileou E, Psycharis IN. Finite element analysis of the seismic response of ancient columns. Earthq Engng Struct Dyn 2019;48:1432–50. https://doi.org/10.1002/eqe.3207.
[59] McKenna F., Fenves G.L., Scott M.H. OpenSees: Open System for Earthquake Engineering Simulation. Pacific Earthquake Engineering Research Center. University of California,Berkeley, CA. Available at: ⟨http://opensees.berkeley.edu⟩ 2000.
[60] Lignos D.G., Krawinkler H. A steel database for component deterioration of tubular hollow square steel columns under varying axial load for collapse assessment of steel structures under earthquakes. Proceedings of the 7th International Conference on Urban Earthquake Engineering (7CUEE) & 5th International Conference on Earthquake Engineering (5ICEE), Tokyo, Japan: 2010.
[61] Ibarra LF, Krawinkler H. Global collapse of frame structures under seismic excitations. Stanford. CA: The John A. Blume Earthquake Engineering Center. Department of Civil and Environmental engineering. Stanford University,; 2005.
[62] Ibarra LF, Medina RA, Krawinkler H. Hysteretic models that incorporate strength and stiffness deterioration. Earthq Engng Struct Dyn 2005;34:1489–511. https://doi.org/10.1002/eqe.495.
[63] Kecman D. Bending collapse of rectangular and square section tubes. Int J Mech Sci 1983;25:623–36. https://doi.org/10.1016/0020-7403(83)90072-3.
[64] Ibarra LF, Krawinkler H. Global collapse of frame structures under seismic excitations. Stanford. CA: The John A. Blume Earthquake Engineering Center. Department of Civil and Environmental engineering. Stanford University,; 2005.
[65] Haselton C.B., Deierlein G.G. Assessing Seismic Collapse Safety Of Modern Reinforced Concrete Moment Frame Buildings. Stanford CA: The John A. Blume Earthquake Engineering Center. Department of Civil and Environmental engineering. Stanford University; 2007.
[66] Ricci P, Manfredi V, Noto F, Terrenzi M, Petrone C, Celano F, et al. Modeling and seismic response analysis of italian code-conforming reinforced concrete buildings. J Earthq Eng 2018;22:105–39. https://doi.org/10.1080/13632469.2018.1527733.
[67] Soleimani R, Khosravi H, Hamidi H. Substitute frame and adapted fish-bone model: two simplified frames representative of RC moment resisting frames. Eng Struct 2019;185:68–89. https://doi.org/10.1016/j.engstruct.2019.01.127.
[68] Charney FA. Unintended consequences of modeling damping in structures. J Struct Eng 2008;134:581–92. https://doi.org/10.1061/(ASCE)0733-9445(2008)134:4(581).
[69] Vamvatsikos D, Cornell CA. Incremental dynamic analysis. Earthq Eng Struct Dyn 2002;31:491–514. https://doi.org/10.1002/eqe.141.
[70] Porter K, Kennedy R, Bachman R. Creating fragility functions for performance-based earthquake engineering. Earthq Spectra 2007;23:471–89. https://doi.org/10.1193/1.2720892.
[71] Schultz M.T., Gouldby B.P., Simm D., Wibowo J.L. Beyond the Factor of Safety: Developing Fragility Curves to Characterize System Reliability. Environmental Laboratory (U.S.) and Engineer Research and Development Center (U.S.); 2010.
[72] Fischer K, Viljoen C, Köhler J, Faber MH. Optimal and acceptable reliabilities for structural design. Struct Saf 2019;76:149–61. https://doi.org/10.1016/j.strusafe.2018.09.002.